UNIVERSITY OF
BIRMINGHAM

The Role of Bacterial Pore Forming Proteins in Modulation of Host Cell Function

Nicole Culverhouse

MSc Thesis

October 4, 2016

Supervisor: Professor Timothy J. Mitchell

Second Supervisor: Professor Ian Henderson

Abstract

Streptococcus pneumoniae is a commensal bacterium found in the nasopharynx. Normally this bacterium is harmless but under the right circumstances it can cause invasive disease. Understanding the interactions between *S. pneumoniae* and the various types of host cells that it comes in contact with would be invaluable in discerning how this bacterium causes invasive disease and aiding in developing treatment options such new vaccines and new antibiotics to combat these diseases.

The aim of this project was to investigate how pneumolysin, the pore forming toxin produced by *S. pneumoniae* interacts with the host and the effect it has on host cells. A key aim of this project was to identify the pathways that are triggered in response to damage caused by pores formed from pneumolysin toxin and how these pathways help the cell resist cell death and aid in cell repair. Also of interest were the mechanisms by which pneumolysin aids in adherence to host cells, as invasion through epithelial and endothelial layers is the first step in invasion and subsequently disease.

This project resulted in the purification of various forms of pneumolysin including the wild type and a nonhaemolytic toxoid. These proteins were quality controlled and their lytic effects were tested on lung epithelial cells, a cell type commonly encountered by *S. pneumoniae* in the course of disease. The effects of pneumolysin on the cell tight junction proteins E-cadherin and actin was also assessed. Preliminary results showed that lytic concentrations of pneumolysin affect the tight junction protein E-cadherin leading to its degradation. Different strains of live *S. pneumoniae* were tested on lung epithelial monolayers. It was found that nonencapsulated *S. pneumoniae* were more proficient at adhering and pneumolysin does not significantly increase adherence of the bacteria to lung epithelial cells.

Acknowledgements

I would like to thank my husband Andrew Culverhouse and my daughters Liliana and Kahlan Culverhouse for all of their patience and support during the work, write up and corrections of this thesis.

I would also like to thank my mom and family for their help and support through this process.

I would like to thank all of the people at the University of Birmingham that helped me and gave me the opportunity to study at the IMI. A special thanks to Professor Tim Mitchell for all of his guidance and support and for the chance to work in his laboratory. Thanks to all the members of the Pneumococcal Research Group for taking the time to teach and help me throughout my time at the IMI. Lastly, I would like to thank the Henderson lab for hosting me for the last few months of my experimental work.

Table of Contents

Abbreviations

PLY = pneumolysin

CDC = cholesterol dependent cytolysins

LPS = lipopolysaccharide

TLR = toll like receptor

WTPLY = wild type pneumolysin

GFP = green fluorescent protein

eGFP = enhanced green fluorescent protein

DPBS = Dulbecco's phosphate-buffered saline

PBS = phosphate-buffered saline

WT = wild type

x g = g force

CFU = colony forming unit

ECL = enhanced chemiluminescence

E-cadherin = epithelial cadherin

VE-cadherin = vasoendothelial cadherin

kDa = kilo Dalton

Å = angstrom

TGF-β1 = transforming growth factor beta 1

PKC-α = protein kinase C alpha

ROCK = Rho associated protein kinase

TNF-α = tumour necrosis factor alpha

TIP peptide = synthetic peptide derived from TIP motif of (TNF-α)

RPMI = Roswell Park Memorial Institute media developed by Moore et al.

DMEM = Dulbecco's Modified Eagle Medium

FCS = fetal calf serum

CO_2 = carbon dioxide

OD_{600} = optical density, absorbance at 600nm

EDTA = ethylenediaminetetraacetic acid

dH_2O = distilled water

PFA = paraformaldehyde

DAPI = 4', 6-diamidino-2-phenylinodole, fluorescent nuclear stain ex/em 358/461

Δ6PLY = pneumolysin mutant generated by an amino acid deletion of alanine 146 and arginine 147

Δ6eGFPPLY = pneumolysin mutant generated by an amino acid deletion of alanine 146 and arginine 147 with an added conjugation to enhanced green fluorescent protein

BSA = bovine serum albumin

SDS = sodium dodecyl sulphate

SDS-PAGE = sodium dodecyl sulphate polyacrylamide gel electrophoresis

HRP = horseradish peroxidise

TBST = Tris-buffered saline plus Tween-20

LDH = lactate dehydrogenase

PdB = Pneumolysin with amino acid change W to F at position 433. Also known as F433

DTT = dithiothreitol

Chapter 1: Introduction

1.1 Streptococcus pneumoniae

First isolated in 1881 by both Louis Pasteur and George Sternberg independently, *Streptococcus pneumoniae* (pneumococcus) is a Gram positive, diplococcus with fastidious nutritional requirements [Murray 2009; Mitchell 2010]. The pneumococcus is a facultative anaerobe that has the ability to utilize various types of carbohydrates using oxygen where available or in the absence of oxygen it can switch to generating ATP via the lactic acid cycle [Murray, 2009]. However, as this bacterium lacks catalase which is required to break down the large amounts of hydrogen peroxide generated when performing aerobic respiration, in order to grow and survive, the pneumococcus requires enriched media supplemented with a catalase source, such as blood [Murray, 2009; Pericone 2003].

S. pneumoniae has a genome of about 2 million base pairs with approximately 2200 total genes [Tettelin, 2001]. This bacterium has high genetic variability with only about 1400 of its total genes being shared by all serotypes (Hiller, 2007). One reason for this high variability is the naturally transformable nature of *S. pneumoniae*. The pneumococcus undergoes competent stages during its life cycle and can readily incorporate external DNA into its genome from closely related species [Johnsborg, 2009; Guiral, 2005]. This activity is thought to help the organism in combating host defences and therefore aiding in its capacity to cause human disease [Guiral 2005].

1.1.1 Carriage and Disease

Streptococcus pneumoniae is a common inhabitant of the nasopharynx of humans, especially children [Mitchell, 2010]. To colonize this part of the human body, *S.pneumoniae* utilizes surface proteins called adhesins to allow it to attach to human epithelial cells. Once attached, this bacterium colonizes the nasopharynx as a normal part of the human flora and protects itself from being physical removed by mucus using its capsule structure [Murray,

2009; Nelson, 2007]. Although *S. pneumoniae* is usually an asymptomatic occupant of the human body it has the capacity to cause invasive disease [Mitchell, 2010]. The pneumococcus causes a variety of illnesses prevalent in children and the elderly including pneumonia, bacteraemia, meningitis and otitis media [WHO, 2012]. An estimated 1 million children die of pneumococcal disease every year with the majority of fatalities occurring in developing countries. However, a significant disease burden can be seen in developed countries such as the United Kingdom [WHO, 2013]. There is an estimated 40,000 hospitalizations and over 100,000 general practitioner consultations regarding pneumococcal diseases such as pneumonia and otitis media reported to Public Health England every year from England and Wales [Public Health England, 2013].

The ability for the pneumococcus to cause invasive disease is due to a variety of virulence factors possessed by the bacterium [Murray, 2009]. These virulence factors include the pore forming protein pneumolysin, the polysaccharide capsule, LPXTG-anchored surface proteins, the pilus, choline binding proteins, lipoproteins and various other surface proteins [Mitchell, 2010].

1.2 Pneumolysin

Pneumolysin (PLY) is the pore forming toxin produced by *S. pneumoniae* and can be found in almost every clinical isolate of this bacterium. This toxin enables the pneumococcus to lyse all cells with cholesterol containing membranes aiding the ability of the bacterium to cause invasive disease (Mitchell 2010; Mitchell 2006). PLY belongs to the family of proteins known as the cholesterol dependent cytolysins (CDC) (Marriot, 2008). This family of proteins mainly includes toxins expressed from a variety of Gram positive bacteria (Cassidy, 2013; Marriot, 2008). The CDC proteins are all soluble monomers that form large, β-barrel pores once they bind to their host cell membrane; however, each one plays a different role in invasive disease that is specific to the bacterium that produces it (Cassidy, 2013). Some

examples of CDCs are listeriolysin O from *Listeria monocytogenes*, streptolysin O from *Streptococcus pyogenes* and perfringolysin O from *Clostridium perfringens* (Gonzalez, 2007).

PLY is a 53kDa asymmetric protein with four domains that forms large pores of 35 to 50 monomeric units with diameters in the size range of 250 to 300Å [Marshall, 2015; Morgan, 1994; Cassidy, 2013]. The mechanism by which PLY forms pores remains undetermined but there is a proposed mechanism which is widely accepted. This mechanism of pore formation begins with the monomer of PLY binding to the host cell membrane, PLY monomers then aggregating together forming a 'pre-pore' complex. The monomers then undergo a change in conformation allowing for insertion into the host cell lipid bilayer (Marriott, 2008; Tilley, 2005). Tilley et al. 2005 used cryo electron microscopy to help support this method of pore formation by taking snapshots of various conformational changes of PLY when it interacts with liposomes.

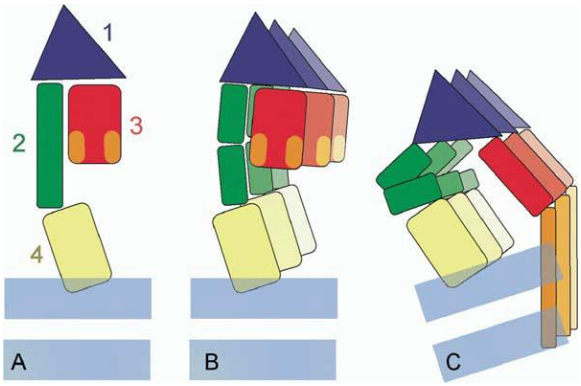

Figure 1.1. Representation of the major stages of pore formation. A) Toxin monomer binding to host membrane. B) Monomers aggregate together forming a 'pre-pore' complex C) Conformational change of the toxin monomers inserting into the host membrane. Figure obtained from Tilley et al. 2005.

Additional support came when PLY was crystallized in two separate studies (Lawrence, 2015; Marshall, 2015). The crystal structure supports the theory of the pre-pore complex as the monomers in the crystal pack side by side and the intermolecular contacts are critical for the haemolytic function of PLY (Marshall, 2015). Two potential binding sites were proposed in the Lawrence et al study (2015). One potential site is located at the base of the 4th

domain while the other is located at the interface of the 3rd and 4th domains at the opposite end of domain 4 (Lawrence, 2015). The exact binding site and mechanism is still to be confirmed.

1.2.2 Release of Pneumolysin

The mechanism of release of pneumolysin from the bacterial cytoplasm is still undetermined as it lacks an N-terminal secretion sequence (Marriot, 2008). This sequence which is present in all of the other CDC family members is essential for the transport of these toxins out bacterial cells while leaving the cell intact (Benton, 1997). PLY is known to be released from *S. pneumoniae* when the bacteria undergoes autolysis during the late log phase of its growth cycle, however this is not the only mechanism of release as other studies have shown haemolytic effects on red blood cells in LytA and LytC autolysin negative mutants (Benton, 1997; Balachandran, 2001; Guiral, 2005).

1.2.3 Effects of Pneumolysin on the Host

Pneumolysin affects the host in both lytic and sublytic concentrations causing the creation of reactive oxygen intermediates, activation of the immune system and activation of various signalling pathways (Mitchell, 2010; Cockeran, 2001; Marriot, 2008).

1.2.4 Pneumolysin and the Host Immune System

The activation of the host immune system by PLY is suggested to aid the bacterium in its colonization of the nasopharynx. As there are many species competing for this niche environment, the ability of *S.pneumoniae* to trigger the host immune system can give the pneumococcus a competitive advantage by clearing other bacterial species while it utilizes its polysaccharide capsule to avoid being cleared itself (Marriot, 2008).

PLY activates the classical complement pathway of the immune system by binding the Fc portion of immunoglobulin and C1q (Paton, 1984; Mitchell, 1991). At the same time, an innate immune response is triggered in the host when PLY binds to the Toll like receptor 4 (TLR4) which is found on the cell surface of macrophages (Srivastava, 2005; Koppe 2012).

Although TLR4 is more commonly associated with LPS in Gram negative bacteria, *in vivo* studies using TLR4 deficient mice found an increased susceptibility to pneumococcal colonization, higher bacterial loads and a dramatic overall reduction in the ability of the host to cope with pneumococcal infection suggesting that TLR4 also plays a role in the infection process of *S. pneumoniae* (Koppe, 2012; Malley, 2003). The interaction of pneumolysin with TLR4 has been suggested to activate the TLR4-dependent caspase-1 pathway. This pathway leads to the production of caspase-1 cytokines such as interleukin (IL)-1α, IL-1β and IL-18 which are involved in cell signalling (Shoma, 2008; Koppe, 2012).

PLY also activates T-cells which contribute to the host's innate and adaptive immune responses. T-cells have been shown to contribute early in the immune response by clearing *S. pneumoniae* (Koppe, 2012; Kadioglu, 2004; Rossum 2005).

Various cell signalling pathways are activated in the presence of PLY. However, whether a pathway is activated by sublytic concentrations of PLY or whether the pathway is triggered by the after effects of host cell lysis is often hard to determine. One such example is the p38 MAPK pathway. When pneumolysin binds to cholesterol, the cell membrane depolarizes too early causing the formation of micropores in the plasma membrane (Iliev, 2007). The micropores are large enough that calcium ions can enter the cell resulting in the activation of various signalling cascades such as the p38 MAPK pathway (Iliev, 2007; Ratner, 2006). However, calcium influx is not the only trigger for the p38 MAPK pathway, as this pathway has also been shown to activate in response to the osmotic stress when PLY forms a mature pore and water subsequently floods into the cell (Ratner, 2006).

1.3 Tight Junctions and E-cadherin

One of the first defences the body has against pathogens is epithelial cell barriers. In order to form a functional seal to prevent invasion into the bloodstream or surrounding tissues, epithelial barriers require both tight junctions and adherens junctions. The interactions

of proteins in these junctions, such as E-cadherin and catenins and their subsequent interactions with the actin cytoskeleton are critical for the successful cell to cell adhesion, intracellular and intercellular signalling (Tian, 2011).

Cadherins are a family of cell surface proteins that function in signalling and regulation of a variety of cellular processes including cytoskeleton remodelling, Rho GTPase cascades, gene expression, membrane trafficking, growth factor signalling, cell motility and proliferation (Saito, 2012; Tian, 2011). The cadherin family of proteins is further split into the classical cadherin group and the desmosomal cadherin group (Saito, 2012). The classical cadherins are then categorized as either type I cadherins or type II cadherins. Type I cadherins include epithelial (E), placental (P) and neural (N) cadherins. Type II cadherins include vasoendothelial (VE), kidney (K) and muscle (M) cadherins (Saito, 2012; Tian, 2011). The classical cadherin, known as E-cadherin or CDH1, is an essential component for the creation and maintenance of a solid and polarized epithelium. The classical cadherins share a single transmembrane structure that utilizes calcium ions to aid in cell to cell adhesion within tissues (Tian, 2011). The cytoplasmic side of the classical cadherins bind to p120 catenin and β-catenin which are members of the catenin family of proteins (Menke, 2012; Saito 2012).

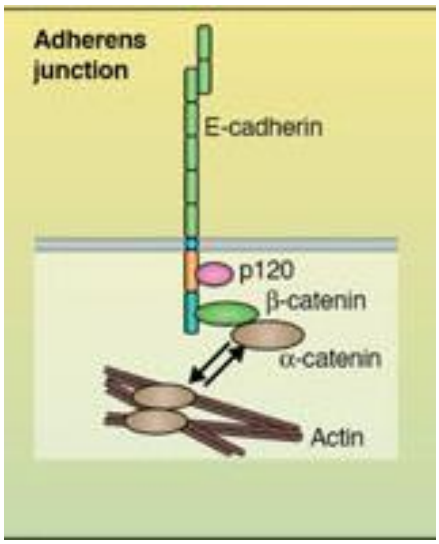

Figure 1.2: Structure of classical cadherins and their binding partners. Figure obtained from Saito et al. 2012.

Interactions between catenins and cadherins play a role in cell to cell adhesion and epithelial morphology. The coupling of β-catenin and E-cadherin is one example. The E-cadherin/β-catenin complex is a critical component in the formation of adherens junctions. If this complex breaks down, for example if β-catenin is phosphorylated, cell-cell adhesion decreases which

in turn leads to increased invasion and migration of cells (Tian, 2011). The breakdown in the E-cadherin/β-catenin complex has been linked to transforming growth factor (TGF)-β1 which is known to act via Snail and/or Smad3 causing a disassociation of the E-cadherin/β-catenin complex (Shao, 2011). TGF-β1 and its role in barrier disruption has been further investigated for its role in bacterial infection in studies such as Beisswenger (2007) and Clarke (2011) which linked this growth factor its downstream pathways to *S. pneumoniae* transepithelial migration (Beisswenger, 2007; Clarke, 2011; Tian, 2011). Whether the bacterial trigger for TGF-β1 signalling is via TLR2, which would point to a reaction to bacterial cell wall components, or TLR4, which may indicate the involvement of pneumolysin is still in debate (Koppe, 2012; Clarke, 2011; Beisswenger, 2007). A study by Inoshima et al. (2011) exposed A549 lung epithelial cells to the small bacterial pore forming protein α-hemolysin from *S. aureus*. This study found a few pore forming toxins led to the degradation of tight junctions in A549 lung epithelial cells by utilizing the host zinc metalloproteinase ADAM10 as a receptor leading to the cleavage of E-cadherin. These results suggest that pore forming toxins may manipulate innate host pathways to serve in invasion and infection (Inoshima, 2011). Other proposed regulators of E-cadherin that may aide in barrier breakdown include PAK1 which is thought to be activated by Rac1 (Menke, 2012). Rac1also works to activate the p38 cascade, which is indicated in the literature to lead to membrane degradation and subsequently *S. pneumoniae* translocation (Clarke, 2011; Beisswenger, 2007; Menke, 2012).

The actin cytoskeleton is associated with tight junctions through the interaction of β-catenin, E-cadherin and α-catenin, another member of the catenin family, (Menke, 2012). TGF-β1 signalling may be located upstream of the Rho GTPase RhoA which acts on the actin cytoskeleton causing cellular morphological changes and leading to the reorganization of F-actin (Shao, 2011).

Rho GTPases act via various signalling pathways to aid in the maintenance of cellular integrity by associating cell junction formation and maintenance with actin cytoskeletal rearrangements. Rho GTPases are key mediators of actin cytoskeleton organization, adherens junction formation and epithelial morphology. The main Rho GTPases involved in the cell junction and cytoskeletal processes are Cdc42, Rac1 and RhoA (Menke, 2012; Shao, 2011). These GTPases have been shown to regulate actin remodelling processes such as membrane ruffling and stress fibre formation that are known to play a role in host invasion by leading to the uptake of bacteria like *Listeria monocytogenes* and *S. pneumoniae* (Menke, 2012; Braun, 1999;Yamaguchi, 2013). Cdc42 is involved with the cytoskeleton and is known to interact with E-cadherin to induce a polarized phenotype in epithelial cells (Desai, 2009). This GTPase also works to control junction integrity by regulating the interaction of junction molecules with the actin cytoskeleton. Activation of Cdc42 leads to the recruitment of E-cadherin and filamentous actin to cell to cell junctions. When E-cadherin arrives at these junctions it forms new contacts and this leads to junction formation. The formation of new junctions activates Rac1 leading to an increase in the formation of E-cadherin contacts and resulting in stronger cell-cell junctions (Menke, 2012). Cell junction integrity is further strengthened through actin polymerization which is initiated thru signalling pathways triggered by the interaction of Rac1 with PAK kinases (Zhao, 1998). The Rho GTPases, Cdc42 and Rac1 have been shown to link E-cadherin ligation to cell survival via Stat3 pathways resulting in an anti-apoptotic signal (Arulanandam, 2009).

1.3.1 Pneumolysin and Tight Junction Integrity

PLY is considered one of the main virulence factors of *S. pneumoniae* and is expressed in almost all clinical isolates. This fact has led to it being implicated as a major player in the progression of *S. pneumoniae* from a harmless commensal to a pathogen causing invasive disease. The exact role of PLY in invasion is hard to determine as varying

concentrations of this toxin encounter many types of host cells and environments making isolating the exact pathways and signalling cascades triggered by PLY difficult. It is likely that PLY triggers multiple signalling cascades that work in tandem to allow for the invasion of this bacterium in a host environment. Inoshima et al. (2011) found some PLY concentrations led to E-cadherin cleavage in A549 cells. However, it was suggested that the cleavage have been triggered by apoptotic pathways rather than the ADAM10 mechanism, which is involved in E-cadherin cleavage when cells were exposed to α-hemolysin, as the E-cadherin was shown to be cleaved only when the A549 cells were exposed to lytic concentrations of PLY (Inoshima, 2011). The serine threonine specific protein kinase PKC-α has roles in the epithelium and may also aid in the invasion of *S. pneumoniae*. Increased PKC-α activity has been shown to lead to the decreased ability of tight junctions to form proper barriers. This kinase has an unusual mode of regulation that is controlled by the plasma membrane. The activity levels of this kinase are influenced by plasma membrane characteristics such as the length of the hydrophobic domain and the fluidity of the lipid bilayer. Low concentrations of diacylglycerols and the ions calcium and magnesium cause increased fluidity and short hydrophobic domains within the plasma membrane leading to an increase in PKC-α activity (Micol, 1999). Lucas et al (2012) showed that sublytic concentrations of PLY led to activation of PKC-α within 30 minutes of exposure (Lucas, 2012). It may be that the activation is due to the insertion of PLY monomers in the lipid bilayer causing a disturbance in fluidity. PKC-α activation could also be the result of changing calcium concentrations within the cell as PLY pores are large and allow calcium ions to flood into a cell but as pores are also rapidly repaired it is not a steady influx. Capillary leakage by PLY exposure was found to be decreased when the PKC-α inhibitor Ro32-0432 is applied. The alveolar epithelial barrier was found to be significantly inhibited *in vivo* with PKC-α activity (Lucas, 2012). TLR4 may also have roles in tight junction integrity

as a study by Wardill et al (2013) describes how TLR4 leads to a change in tight junction integrity through the initiation of PKC activity in gut epithelial cells (Wardill, 2013). PKCs may be involved with the breakdown of tight junctions in other types of epithelial cells leading to *S. pneumoniae* invasion into the bloodstream.

Another hypothesis for PLY role in invasion centres around its effects on the actin cytoskeleton and intercellular junctions. Effects on these systems have been investigated in neuronal cells and endothelial cells. The activation of two small GTPases, Rac1 and RhoA, occurred when astrocytes were exposed to sublytic concentrations of PLY, (Hupp, 2012). Both Rac1 and RhoA have been linked to regulation of the actin cytoskeleton through cell movement or the formation of stress fibres respectively. Rac1 aids in the formation of lamellipodia and may utilize calcium in its activation as the activation of Rac1 by PLY is inhibited when calcium free buffer is used. RhoA aids in the formation of stress fibres, an effect that seems to be regulated through the usual RhoA to Rho associated protein kinase (ROCK) pathway. Evidence of this is found when treatment with a ROCK inhibitor negates the increase in stress fibres found in an uninhibited system. Unlike Rac1, RhoA does not seem as dependent on calcium as its induction was similar regardless of the concentration or presence of calcium in the buffer (Iliev, 2007). How these GTPases aid in invasion is seen when the effects Rac1 and RhoA have on cell barriers comes into play. Rac1 has been shown to be cell barrier protective while RhoA has been shown to be cell barrier disruptive. When cells are exposed to PLY an imbalance of these two proteins occurs. The negative effects of the GTPase imbalance have been shown to be reduced when cells are treated with an inhibitor of PKC-α, TIP peptide, which mimics the lectin like domain of TNF-α (Lucas, 2012). A study of the blood brain barrier implicated the RhoA/ROCK pathway as having an effect on the GTPase imbalance and subsequently disrupting the protective nature of cell barriers. This study found that the RhoA/ROCK pathway triggered phosphorylation of myosin light chain

which also occurs when cells are treated with PLY (Srivastava, 2013; Lucas, 2012). Srivastava et al also found that the myosin light chain phosphorylation led to the breakdown of occludin which is one of the main components of tight junctions (Srivastava, 2013). This brings the question of whether PLY-induced activation of the RhoA GTPase pathway also leads to the disruption of occludin which could result in the invasion of pneumococci from the nasopharynx to the blood or CSF due the dysfunctional tight junctions. Evidence for a direct relationship between PLY and VE-cadherin was found when lung endothelial cells were treated with sublytic concentrations of PLY. PLY treatment for 2 hours led to a significant decrease in VE-cadherin resulting in an increase in gap formation. The monolayer integrity was rescued when TIP peptide was applied. This evidence again links TNF-α and RhoA/Rac1 to the story of cell barrier dysfunction (Lucas, 2012). PKC-α has also been linked with RhoA/Rac1 and may prove to be an upstream member of this pathway providing a bridge between extracellular PLY and intracellular signalling (Lucas, 2012).

Pneumolysin, the pore forming toxin of *Streptococcus pneumoniae,* and a member of the CDC protein family is an important factor in causing invasive disease in human hosts. This protein has been linked to many signalling cascades that are associated with the formation and integrity of epithelial cell barriers but has not been directly linked to the cleavage of E-cadherin or another epithelial cell protein that would allow the passage of *Streptococcus pneumoniae* into the host. One of the aims of this project was to look into these pathways and see if there is any connection between PLY and a disruption of the epithelial cell barriers.

1.4 Aims and Objectives

The aim of this Masters project was to investigate the various effects of pneumolysin on host cells and to try to identify host-pathogen interactions that could contribute to the switch from harmless commensal to invasive disease with the main focus on epithelial cell

barriers. The toxin was tested on lung epithelial cells to assess the damage caused under various concentrations of toxin.

A specific objective was to determine if the toxin pneumolysin has any effect on adherence of the bacterium to its host as pneumolysin is present in almost every case of clinical disease caused by *S. pneumoniae*. This led to investigating the degradation of E-cadherin when lung epithelial cells were exposed to the pneumolysin toxin. The Inoshima group (2011) investigated the zinc metalloproteinase ADAM10 pathway and discovered that it led to degradation of E-cadherin when A549 lung epithelial cells were exposed to another pore forming toxin, α-hemolysin. The observation by this group led to one of the key questions in this project, is E-cadherin degraded by the ADAM10 pathway when A549 cells are exposed to pneumolysin as it is when they are exposed to α-hemolysin? There is already evidence of some activation of the ADAM10 pathway with pneumolysin. But as pneumolysin is a large pore forming protein whereas α-hemolysin is a small pore forming protein, the question remains of whether an influx of calcium ions trigger the normal cellular apoptotic pathways leading to the degradation of E-cadherin is the mechanism followed in *S. pneumoniae*-host interactions. This apoptosis driven alternative hypothesis is supported by evidence of E-cadherin degradation when pneumolysin is present in lytic but not sublytic concentrations.

Another question raised by previous studies was whether the morphological changes to the cytoskeleton that occur in the host when exposed to pneumolysin were cause by a direct interaction between the toxin and actin or whether the toxin instead triggers Rho GTPase signalling pathways within the host which lead to the observed morphological changes in the cytoskeleton. These cytoskeletal changes could be another pathway which aid in streptococcal invasion in the host. This line of investigation was inspired by the work of the Iliev group (Iliev, 2007; Hupp, 2012).

Other preliminary objectives of this project included investigating the localisation of pneumolysin by producing a fluorescent tagged, endogenously produced toxin and producing a chemically defined media which could be used in studies that focus on the host cell repair mechanisms. The ability to remove ions such as calcium would highlight the importance of these ions and the pathways in which they are involved in the cell choice between repair and apoptosis.

In summary, this study was interested in purifying wild type pneumolysin and a nonhaemolytic toxoid in order to determine if invasion of the host by *S. pneumoniae* is enhanced by the pore forming toxin pneumolysin and whether or not pneumolysin plays a key role in adherence of *S. pneumonaie* to the host.

Chapter 2: Methods and Materials

2.1 Protein Purification

2.1.1 Purification of pneumolysin

E. coli containing pET-33BPLY plasmid for expression of His-tagged pneumolysin were grown overnight in LB broth (Sigma) + 50µg/ml kanamycin (Sigma). Four flasks of 1L of LB broth + 50µg/ml kanamycin each were then inoculated with 10ml of overnight culture each. *E. coli* was allowed to grow at 37^{o}C whilst shaking until OD_{600} 0.8 was reached. A concentration of 1mM IPTG (Fisher) was then added to each flask. Cultures were allowed to grow for another 3 hours before cells were collected by centrifugation at 3220 x g for 25 minutes at 4^{o}C and the pellet resuspended in 5ml of PBS per litre of culture. The pellet was frozen at -20^{o}C with protease inhibitors (Roche), DNase 1 (Sigma), and benzamidine (Sigma) to prevent any degradation. The pellet was then thawed on ice before disrupting the cells using the one shot cell disrupter set to 12k PSI. The disrupted cells were then centrifuged at 18000 x g for 40 minutes at 4^{o}C to remove debris. The lysate (supernatant) was then run through a 5ml nickel affinity column to load the protein. Nickel Affinity Chromatography by imidazole (Acros Organics) gradient was then performed using the Akta Primeplus (GE). Fractions were run on SDS-PAGE and stained with Coomassie blue to determine fractions to be pooled and dialysed using dialysis tubing in 2L of Anion Exchange wash buffer for at least 24 hours. Dialysed protein was loaded by recirculation through an Anion Exchange column for at least 20 minutes on ice on loop to load the column. Protein then underwent Anion Exchange Chromatography by NaCl (Merck) gradient using the Akta Primeplus. Fractions were again run on SDS-PAGE and stained with Coomassie blue to determine fractions to be pooled. Dialysis was performed in 2L of 1x sterile PBS pH 7.4 for at least 24 hours before being changed to 2L of fresh 1x sterile PBS and left for another 24 hours. Protein was then collected and the concentration measured on the ND-1000 Nanodrop. Protein was diluted to

as close to 1.0 mg/ml as possible by very slowly adding 1x sterile PBS before aliquoting and freezing down into the -20^{o}C and -80^{o}C freezers for future use.

2.1.2 Protein purification of Δ6PLY and eGFPΔ6PLY

Δ6PLY is a pneumolysin mutant that was created by an amino acid deletion of the amino acids alanine 146 and arginine 147 leading to a nonhaemolytic version of the toxin. The monomers of Δ6PLY attach to the membrane but the protein cannot complete the conformational change required to insert into the host membrane.

E. coli containing pET-33BΔ6PLY plasmid (Kirkham 2006) for expression of his-tagged Δ6PLY protein or *E. coli* containing pET-33BeGFPΔ6PLY (Cowan 2006) plasmid for expression of his-tagged, eGFP fluorescence conjugated Δ6PLY protein were grown overnight in LB broth (Sigma) + 50μg/ml kanamycin (Sigma). Four flasks of 1L of LB broth + 50μg/ml kanamycin each were then inoculated with 10ml of overnight culture each. *E. coli* was allowed to grow at 37^{o}C whilst shaking until OD_{600} 0.8 was reached. A concentration of 1mM IPTG (Fisher) was then added to each flask. Cultures were allowed to grow for another 3 hours before cells were collected by centrifugation at 3220 x g for 25 minutes at 4^{o}C and the pellet resuspended in 5ml of PBS per litre of culture.

Purification proceeded as per section 3.1.1 above.

2.1.3 Generation of Negative Vehicle for Purified Pneumolysin

A negative control, termed vehicle, was made from the solvent fraction of the PLY preparation without the toxin. To generate a negative vehicle, pneumolysin was absorbed from the buffer using affinity chromatography. 200μl of nickel magnetic beads (Millipore) to bind to the His tag of the PLY toxin were added to a 1.5ml microcentrifuge tube and placed in a magnetic rack. The storage solution was removed and the beads washed in 200μl of DPBS, after which 200μl of purified WTPLY NC-01 was added to the beads. The toxin and beads were mixed by pipetting and the 1.5ml microcentrifuge tube was placed on a shaker for 1 hour

at room temperature. To retrieve the negative vehicle, the 1.5ml microcentrifuge tube was placed back on the magnetic rack and the supernatant transferred to a new 1.5ml microcentrifuge tube.

2.1.4 Generation of Nickel Elution Protein for Purified Pneumolysin

To generate the nickel eluted protein, 200µl of nickel elution buffer, buffer containing imidazole used to elute the protein of interest from the nickel chromatography column was added to the nickel magnetic beads after the negative vehicle was removed. The beads and buffer solution was mixed by pipetting in a 1.5ml microcentrifuge tube and placed on an orbital shaker (Orbital Shaker S03 Stuart Scientific) for 1 hour at room temperature. To retrieve the nickel eluted protein, the 1.5ml microcentrifuge tube was placed back on the magnetic rack and the supernatant transferred to a new 1.5ml microcentrifuge tube.

2.2 Cell Based Assays

2.2.1 Haemolytic assay

In duplicate, 50µl of a positive control (lab stock pneumolysin, 1µg/ml), the newly purified pneumolysin (batch NC-01, 1µg/ml) and negative vector (magnetic Ni bead flow through, neat) were serially diluted in 50µl of DPBS (Sigma) across the rows of a 96 well round bottom plate (Sarstedt) To each well, 50µl of 10Mm DTT (Melford) diluted in DPBS was added. The 96 well plate was covered and allowed to incubate at 37^{o}C for 15-30 minutes. During incubation, 1ml of sheep blood (E&O Laboratories) was centrifuged to collect erythrocytes in a pellet discarding the supernatant. Cells were washed until the supernatant was clear. The cleaned erythrocytes were diluted into a 2% solution in DPBS. After the incubation time, 50µl of 2% erythrocyte solution was added to each well and the plate was covered and allowed to incubate at 37^{o}C for 30 minutes. After the incubation, 50µl of DPBS was added and the plate was centrifuged for 1 minute at 138 x g (Eppendorf) to collect the remaining erythrocytes in pellets at the bottom of each round well. After spinning, 100µl of

supernatant was transferred from each well to a new flat bottom 96 well plate (Falcon) and absorbance 540nm was measured in a plate reader (BMG Labtech Omega Fluorostar) to analyse lysis.

2.2.2 Lactate Dehydrogenase (LDH) Assay

The results of the LDH assay indicate membrane permeability as LDH is small enough to escape through the large pore formed by PLY. L929 fibroblast cells were seeded into a 96 well plate (Falcon) at a concentration of 6×10^4 cells/well. After overnight incubation to allow cells to attach, all supernatant was removed from the wells and replaced with media (RPMI 1640 (Sigma), 10% FCS (Labtech), 1% L-glutamine (Sigma), 1% penicillin/streptomycin (PAA)) containing the appropriate concentrations of WTPLY NC-01 (10µg/ml, 0.5µg/ml, 0.1µg/ml, and 0.05µg/ml diluted in RPMI media), negative vehicle (same volume added as the WTPLY concentrations), or media alone in triplicate. Cells were incubated for 37^{o}C and 5% CO_2 in conditions for 3 or 6 hours before the supernatant was removed for the assay. Supernatant processing, lysis control, and positive control were done following the manufacturer's instructions. LDH assay kit used was Promega Cytotox 96 Non-Radioactive Cytotoxicity Assay.

2.2.3 MTT (3-(4, 5-Dimethylthiazol-2yl)-2, 5-diphenyltetrazolium bromide) Assay

The results of the MTT assay indicate live or dead cells. L929 fibroblast cells were seeded into a 96 well plate (Falcon) at a concentration of 6×10^4 cells/well. After overnight incubation to allow cells to attach, all supernatant was removed from the wells and replaced with media (RPMI 1640, 10% FCS, 1% L-glutamine, 1% penicillin/streptomycin; Sigma) containing the appropriate concentrations of WTPLY NC-01 (10µg/ml, 0.5µg/ml, 0.1µg/ml, and 0.05µg/ml in RPMI), negative vehicle (same volume added as the WTPLY concentrations), or media alone in triplicate. Cells were incubated for 37^{o}C and 5% CO_2 in conditions for 3 or 6 hours before the supernatant was removed. After exposure time, 50µl of

MTT stain (Thiazolyl Blue Tetrazolium Bromide (Sigma) diluted in Dulbecco's PBS (Sigma)) was added to each well. Cells were incubated at 37^{o}C, 5% CO_2 for a further 4 hours. After incubation all liquid was removed and 100µl of MTT solvent (40µl HCl n 10ml isopropanol) was added to each well. Liquid was mixed using an orbital shaker for 2 minutes at 150 RPM. Absorbance was read in a plate reader at a wavelength of 540nm.

2.3 Host-pathogen interactions

2.3.1 Growth curves

Standard inocula were used for growth curves so that the CFU/ml and OD_{600} of the bacteria were constant. Strains used were WT D39 and WT TIGR4 *Streptococcus pneumoniae* lines (see Appendix II: Strains used in this study for further details). Standard inocula were retrieved from the -80 freezer and quick thawed in a 37^{o}C water bath. They were transferred to a 1.5ml microcentrifuge tube and centrifuged at 3200 x g for 5 minutes. Pellets were washed twice in 1x sterile PBS before use. Both strains at OD_{600} 0.3 were added to a 96 well flat bottom plate (Falcon) at 0.15 CFU/ml in triplicate in both BHI (Oxiod) and CDM media. Media alone served as negative controls and blanks. The 96 well plate was covered and allowed to incubate in the plate reader for 18 hours under normal atmospheric conditions reading every 30 minutes. During the plate reader experiment, duplicate cultures of 10ml of BHI or CDM and 0.15 CFU/ml of each bacterial strain per condition were allowed to grow under atmospheric conditions in a 37^{o}C water bath. Every hour for the first 4 hours of growth a 1ml sample from each strain in each condition was taken and OD_{600} measured. Samples were centrifuged for 5 minutes at 3200 x g. Pellet was washed twice and resuspended in sterile PBS. Viable counting was done in duplicate with triplicate spots for each sample to more accurately determine growth in CFUs/ml.

2.3.2 Transformation of *E. coli*

A 100µl aliquot of XL1-Blue competent *E. coli* was taken from the -80^{o}C freezer for each condition. The aliquot was allowed to thaw on ice before 1ml of plasmid DNA pJWV25 was added and incubated for 20 minutes on ice before being transferred to a chilled 0.1cm electroporation cuvette (Cell Projects). Electroporation was accomplished using the following settings: 2.5Kv, 25mF, and 200Ω (GenePulsar Electroporator). The cuvette was returned to ice and 200ml of room temperature SOC media was added. Samples were then transferred to a microcentrifuge tube and incubated for 1 hour at 37^{o}C. Various volumes of sample were plated on LB agar + 100µg/ml of ampicillin (Sigma). Plates were incubated overnight at 37^{o}C and checked for colonies the following day.

2.3.3 Plasmid DNA preparation

Plasmid DNA was prepared using 5ml of overnight culture of *E. coli* in LB broth + ampicillin (Sigma) for pJWV25 plasmid and the Qiagen Spin Miniprep Kit (QIAGEN). The manufacturer's instructions were followed choosing the optional step and elution in 30ml of molecular grade dH_20 (Sigma).

2.3.4 Transformation of *S. pneumoniae*

S. pneumoniae D39 was grown on a blood agar plate (BAB No. 2 (Oxoid) + 5% Horse blood (E&O Laboratories)) overnight at 37^{o}C and 5% CO_2. The following day, 10ml of sterile BHI (Oxoid) was inoculated with a loopful of D39 from the blood agar plate and allowed to grow overnight at 37^{o}C and 5% CO_2. The next day, 30ml of sterile BHI + 1mM $CaCl_2$ (BDH) was inoculated with 500µl of overnight culture and incubated until an OD_{600} of 0.1 to 0.3 was reached. For each transformation, 1ml of culture and 100ng/ml CSP-1 were added into a 1.5ml microcentrifuge tube. Cultures were incubated in a 37^{o}C water bath for 15 minutes. The plasmid of interest or a control plasmid with the desired antibiotic resistance was added to each respective culture and cultures were incubated for a further 1 hour 15 minutes in a 37^{o}C water bath. A 300µl aliquot of each culture was spread onto respective BAB plates and

allowed to incubate at 37°C and 5% CO_2 overnight. Any colonies were picked and replated onto antibiotic plates to test for selection.

2.3.5 Extraction of genomic DNA from bacteria

Genomic DNA was extracted using the (Nexttec). Solutions were made fresh per sample are as shown in the table below and were mixed by pipetting before use:

Solution Name	Nexttec Reagent Name	Amounts of Reagents
Lysis Buffer 1 (LB1)	Buffer B1	90µl
	Lysozyme	10µl
	RNase A	20µl
Lysis Buffer 2 (LB2)	Buffer B2	2.5µl
	Buffer B3	10µl
	Purified Dh_20	87.5µl
	DTT	2.5µl
	EDTA	2.0µl

Per sample, 120µl of LB1 were added to a screw cap tube. A generous loopful of bacteria was added to the screw cap tube and mixed with pipetting. To give continuous agitation, samples were incubated in a hybridisation chamber at 60°C for 20 minutes. After initial incubation, 104µl of LB2 was added to each tube and mixed by pipetting. Samples were allowed to incubate in the hybridisation chamber for 60 minutes at 60°C. Columns were prepared by adding 350µl Prep Buffer (Nexttec) to the column and leaving at room temperature for at least 5 minutes. Columns were then centrifuged at 350g for 1 minute. Flow through was discarded and a new microcentrifuge tube was connected to the column. After the hour incubation, the entire sample was pipetted onto the column and left to incubate at room temperature for 3 minutes. The column was centrifuged at 700g for 2 minutes then flow through was collected into a new tube and the concentration measured via Qubit fluorometer (Invitrogen). DNA was stored at -20°C until required.

2.4 Exposure of A549 Lung Epithelial Cells to GFP tagged toxin

2.4.1 Exposure of A549 Lung Epithelial Cells to eGFP tagged PLY toxin

A549 human lung carcinoma epithelial cells were seeded at a density of 7500 cells/well onto a 10mm, size 0, uncoated, sterile coverslip within a 24 well plate (Costar).

Complete Dulbecco's Modified Eagle Medium (DMEM) [see Appendix 1] was added to each well and cells were allowed to incubate at 37°C, 5% CO_2 for 48 hours or until a monolayer formed. After the appropriate incubation time, the media was removed from the well. An eGFP fluorescently tagged version of PLY (eGFPPLY) was added to the monolayers at the following concentrations: 1.1µM, 11.1µM and 111.2µM. The cells and toxin were allowed to incubate for 30 minutes at 37°C and 5% CO_2. After the incubation time the media and toxin was removed and the monolayers were washed in 1ml of warm complete DMEM. Cells were fixed with 3.8% paraformaldehyde (PFA; Affymetrix) in media for 10 minutes at room temperature. After fixation the PFA solution was removed and monolayers were washed 3 times with 1 ml of DPBS each time. Coverslips were then mounted to slides using 2ul of Prolong Gold Antifade Reagent with DAPI (Life Technologies) and sealed with nail varnish. After allowing 24 hours for the slides to dry, coverslips were visualized using confocal microscopy (Nikon A1 Confocal Microscope).

2.4.2 Exposure of A549 Lung Epithelial Cells to eGFP tagged Δ6PLY toxin with Live Cell Imaging

A549 lung epithelial cells were seeded at a density of $2x10^5$ cells/well into a 24 well plate (Costar). Complete Dulbecco's Modified Eagle Medium (DMEM) [see Appendix 1] was added to each well and cells were allowed to incubate at 37°C, 5% CO_2 for 48 hours or until a monolayer formed. After the appropriate incubation time, the media was removed from the well. An eGFP fluorescently tagged version of Δ6PLY (Δ6eGFPPLY) was added to the monolayers at the following concentrations: 1.8µM, 18.1µM and 180.6µM to match the wild type concentrations. The cells and toxin were allowed to incubate for 30 minutes at 37°C and 5% CO_2. After the incubation time the media and toxin was removed and the monolayers were washed in 1ml of warm DPBS. RPMI medium without phenol red (Sigma) supplemented with 1mM sodium pyruvate (Sigma) and 10% FCS (Gibco) was added at a

volume of 1ml to each well and cells were then visualized using confocal microscopy (Nikon A1 Confocal Microscope).

2.5 Immunofluorescence Microscopy

2.5.1 Toxin exposure following by staining for cellular actin

In a 24 well plate (Costar), A549 lung epithelial cells were seeded at a density of 7500 cells/well onto an uncoated 10mm diameter, 0 thickness coverslip. Cells were allowed to grow for approximately 48 hours in complete DMEM media [see Appendix 1] at 37^{o}C and 5% CO_2 until a monolayer was formed. After a monolayer was formed on the coverslip, the media was removed from the well and eGFPPLY toxin diluted in warm, complete DMEM media was added at varying concentrations to the appropriate wells. Cells were incubated for 2 minutes at 37^{o}C and 5% CO_2. The toxin and media were removed from each well and the cells were washed in 1ml warm complete DMEM media. Cells were then fixed by adding 1ml of 3.8% paraformaldehyde (4% PFA; Affymetrix) in complete DMEM media and allowed to incubate at room temperature for 10 minutes. The fixative solution was then removed and the coverslip was washed 3 times with 1ml of warm DPBS (Sigma). Cells were then permeablilized by adding 1ml of 0.1% Triton X-100 (Sigma) diluted in DPBS to the necessary wells and incubated at room temperature for 5 minutes. The next step required the coverslips be washed in 1ml of warm DPBS 3 times. A blocking step was then performed by adding 1ml of 4% BSA (Sigma) diluted in warm DPBS to the coverslips and allowing them to incubate at room temperature for 30 minutes. The coverslips were again washed 3 times in 1ml of warm DPBS before incubating with Phalloidin Alexa Fluor 555 (Life Technologies) diluted 1 in 200 in warm DPBS to stain for F-actin. A final incubation in the phalloidin antibody was performed for 20 minutes at room temperature before the coverslips were washed 3 times with 1ml of warm DPBS. Coverslips were then touched to a paper towel to remove excess DPBS before being mounted onto a slide with 2μL of Prolong Gold Antifade

Reagent with DAPI (Life Technologies) and sealed with nail varnish. Slides were allowed overnight to dry and ensure mount was hardened before visualizing by confocal microscopy (Nikon A1 Confocal Microscope).

2.5.2 E-cadherin staining

In a 24 well plate (Costar), A549 lung epithelial cells were seeded at a density of 7500 cells/well onto an uncoated 10mm diameter, 0 thickness coverslip. Cells were allowed to grow for approximately 48 hours in complete DMEM media [see Appendix 1] at 37^{o}C and 5% CO_2 until a monolayer was formed. After a monolayer was formed on the coverslip, the media was removed from the well and the cells were washed 3 times in 1ml warm DPBS (Sigma). Cells were then fixed by adding 1ml of 3.8% paraformaldehyde (PFA; Affymetrix) in complete DMEM media and allowed to incubate at room temperature for 10 minutes. The fixative solution was then removed and the coverslip was washed 3 times with 1ml of warm DPBS. Cells were then permeablilized by adding 1ml of 0.1% Triton X-100 (Sigma) diluted in DPBS to the necessary wells and incubated at room temperature for 5 minutes. Coverslips were then washed 3 times in 1ml of warm DPBS. Coverslips were then blocked by adding 1ml of 4% BSA (Sigma) diluted in warm DPBS and allowed to incubate at room temperature for 30 minutes. The coverslips were again washed 3 times in 1ml of warm DPBS before incubating with mouse monoclonal E-cadherin primary antibody (Biolegend) at a concentration of 1 in 50 diluted in warm DPBS. The coverslips were allowed to incubate in the primary antibody for 1 hour at room temperature before being washed 3 times with 1ml of warm DPBS. Alexa Fluor 633 anti-mouse secondary antibody (Life Technologies) was then added to the coverslips at a concentration of 1 in 1000 diluted in warm DPBS. Cells were allowed to incubate in the secondary antibody for 1 hour at room temperature before being washed 3 times in 1ml of warm DPBS. Coverslips were then touched to a paper towel to remove excess DPBS before being mounted onto a slide with 2µL of Prolong Gold Antifade

Reagent with DAPI (Life Technologies) and sealed with nail varnish. Slides were allowed overnight to dry and ensure mount was hardened before visualizing by confocal microscopy (Nikon A1 Confocal Microscope).

2.6 Western blotting for E-cadherin

A549 cells were grown to confluent monolayers in a 75cm^2 tissue culture flask (Starstedt). The media was removed and the monolayers were washed once in DPBS (Sigma). Where applicable, wild type pneumolysin was added in the appropriate concentrations in serum-free media. Cells were allowed to incubate for 1 hour at 37^{o}C and 5% CO_2. After the incubation, monolayers were washed once in DPBS and lysis buffer [see Appendix 1] was then applied to each monolayer in an appropriate amount (1ml for 75cm^2 tissue culture flask). Cells were visually checked for lysis using a microscope, ensuring cells had rounded and shrunk down. Once lysis occurred, the lysis buffer combined with cell material was collected and centrifuged at 21728 x g on a benchtop centrifuge (Eppendorf) for 10 minutes to remove cellular debris. After centrifugation, the supernatant was collected and used for SDS-PAGE. For each sample, 9µl of supernatant was added to 3µl of SDS PAGE sample buffer (4x reducing SDS PAGE sample buffer [see Appendix 1]) and heated for 10 minutes at 70^{o}C. Samples were loaded onto a bis-tris gel (NuPAGE 4-12% Bis-Tris Gel, Novex Life Technologies) and ran for 50 minutes at 180 volts. Protein was then transferred to a nitrocellulose membrane for Western blotting (iBlot Gel Transfer Mini Stack, Novex Life Technologies).

For Odyssey visualisation, the membrane was blocked in 3% BSA (Sigma) in TBST [see Appendix 1] for 1 hour at room temperature before primary E-cadherin mouse monoclonal antibody (Biolegend) and anti-actin rabbit polyclonal antibody made to 1in 500 dilution in 3% BSA + TBST and added to the membrane. Membrane was incubated in primary antibody for 16 hours at 4^{o}C. After incubation, the membrane was washed 3 times 10

minutes in high salt TBST [see Appendix 1]. The membrane was then incubated in anti-mouse conjugated 800 and anti-rabbit conjugated 700 secondary antibodies (IRDye secondary antibodies; Licor) at 1:10000 for 1 hour shaking at room temperature. After incubation in secondary, the membrane was washed 5 times 5 minutes in high salt TBST followed by a further 2 washes in TBS [see Appendix 1]. Membrane was dried using Whatman paper and visualised in both the 700nm and 800nm channels of the Licor Odyssey Infrared Imager (Licor).

2.7 Adherence Assay

A549 lung epithelial cells were seeded into a 24 well plate (Costar) at a density of $2x10^5$ cells into 1ml of RPMI medium without phenol red (Sigma) supplemented with 1mM sodium pyruvate (Sigma) and 10% FCS (Gibco). Cells were placed in the incubator at 37^oC and 5% CO_2 overnight to allow for attachment. After overnight incubation, the media was removed from the cells and replaced with fresh media. After a further 24 hour incubation, 48 hours in total, cells were confluent. The media was removed from the wells and the monolayer was washed two times with 2ml of sterile DPBS (Sigma) each time.

Starter cultures of strains of *S.pneumoniae* (FP22, D39, D39 PLY STOP, and R6 see Appendix II: Strains used in this study for further details).at an OD_{600} of 0.6, mid log, were warmed briefly in the water bath before centrifuging at 3200 x g for 5 minutes and washing in 1ml sterile DPBS. This process was repeated for a total of 2 times. The 1ml of bacterial culture was then re-suspended after a final centrifugation into RPMI without phenol red supplemented with 1% FCS. Bacteria were added to each corresponding monolayer at $1x10^7$ CFU/ml per well. The CFU/ml was predetermined by viable counting and was confirmed via a viable count of the starting inoculums for each type of bacteria used. The cells and the bacteria were then incubated for 2 hours at 37^oC and 5% CO_2. After the incubation time, the medium was removed from each well and the monolayer of cells was washed 3 times with

1ml of sterile DPBS. The monolayer was then washed with 200µl of 1x trypsin/EDTA (Sigma) for approximately 10 minutes at 37^{o}C until cells freely detached from the plate. 800µl of ice cold, sterile dH2O was added to lyse the A549 cells releasing the adhered bacteria. The resulting A549 lysate suspension was serial diluted and viable counted. The percent adherence was then calculated using the viable count from the starting inoculums and the final viable count.

Chapter 3: Results

3.1 Protein purification

3.1.1 Purification of the pore forming protein pneumolysin

The first step to testing the effects of pneumolysin on various host cell pathways was to purify and quality check recombinant pneumolysin. To produce large quantities, BL21 *E. coli* expressing the plasmid pET33BPLY, which is the pET33b plasmid with the addition of the PLY gene linked to a His tag were grown and PLY purified as described in section 2.1.1. The His tag was included in this protein to allow for purification via nickel affinity chromatography. The protein was then subjected to anion exchange chromatography to separate the protein of interest from any contaminants such as lipopolysaccharide (LPS) that can occur from producing this protein in *E. coli* rather than its native bacterium S. *pneumoniae*. If LPS remains in the protein preparation the results of cell based assays would be inconclusive as there would be no way to determine if the effect was due to PLY or LPS.

Quality control steps were performed after each stage of purification. Fractions were selected from the peak of the AKTA trace profiles and analysed by gel electrophoresis and western blotting to ensure only the purest and highest concentration protein fractions would be carried to the next step of protein purification (Figure 3.1 for NAC and 3.2 for AEC).

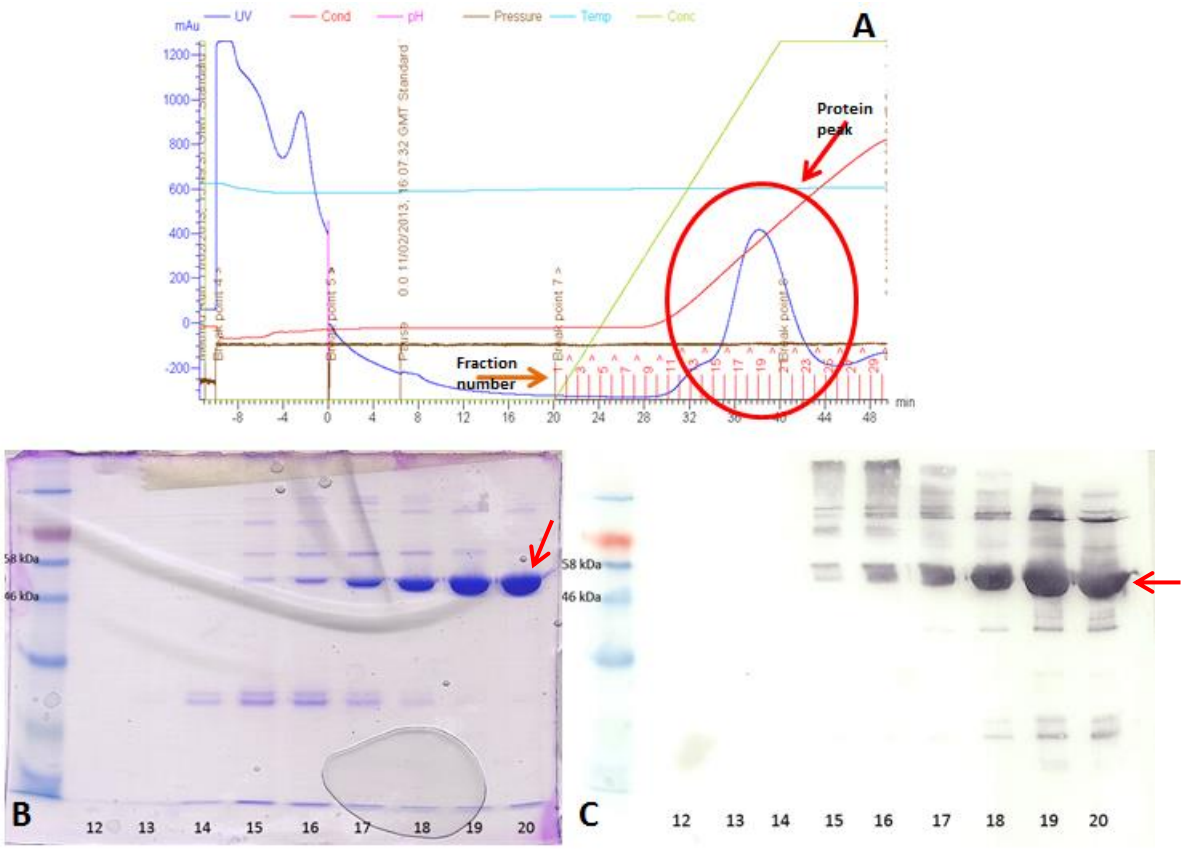

Figure 3.1 Results **of pnuemolysin purification after Nickel Affinity Chromatography A:** AKTA profile showing the protein in each 1ml fraction eluted from the NAC column **B:** Coomassie gel depicting fractions 12-20 diluted 1:10 selected from peak on AKTA trace **C:** Western blot depicting fractions 12-20 diluted 1:10 selected from peak on AKTA trace. Red arrows on Coomassie gel and western blot point to protein of interest, WTPLY at expected molecular weight of 57kDa.

The NAC fractions 18 to 20 were combined for dialysis before continuation to AEC.

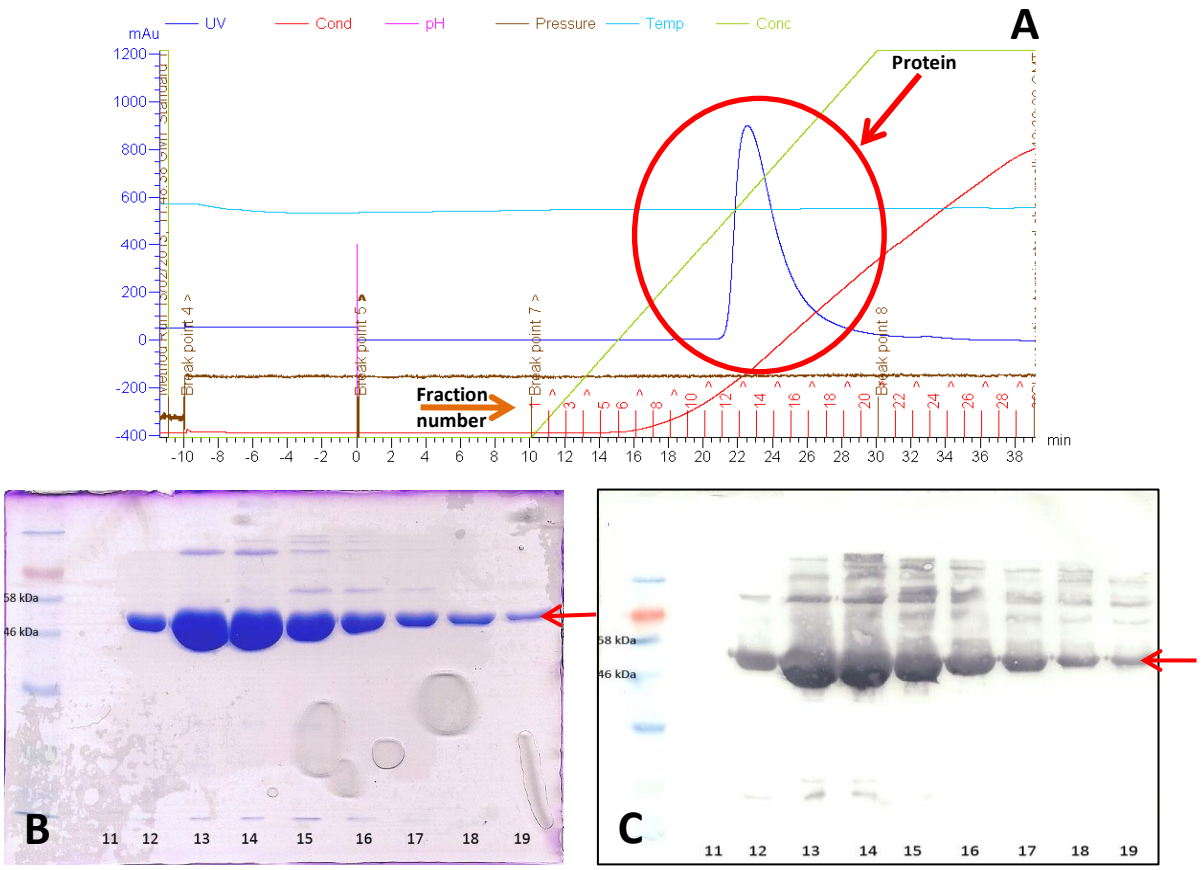

Figure 3.2 Results **of pneumolysin purification after Anion Exchange Chromatography A:** AKTA profile showing the protein in each 1ml fraction eluted from the AEC column **B:** Coomassie gel depicting chosen fractions 11-19 selected from peak on AKTA trace **C:** Western blot depicting chosen fractions 11-19 selected from peak on AKTA trace. Red arrows on Coomassie gel and western blot point to protein of interest, WTPLY at expected molecular weight of 57kDa.

The AEC fractions 12 thru 14 were combined for dialysis and ultimately became the final WTPLY protein. The concentration of the PLY produced was 1.81mg/ml and was given a batch coding of NC-01. A Coomassie gel and western blot were performed in order to ensure the protein purified was pneumolysin and that no contaminants were present (Figure 3.3). The Coomassie gel was used to check for any large contaminants that may have eluded the purification process as Coomassie stains all protein non-specifically. The Coomassie gel run in this case shows a single band for WTPLY NC-01 at a size of 57 kDa. This is the expected size for the recombinant His-tagged pneumolysin. The western blot shows 2 bands, the expected pneumolysin band and a band of a higher molecular weight. The origin of this

band was unknown and was sent for identification via mass spectrometry. Reported results indicated it was a protein found in *E. coli*. As this band was found in all lab preparations of the recombinant PLY it was concluded that this band was most likely found in the original purified WTPLY that was used to create the polyclonal primary antibody used in these western blots and is therefore visible on the blot.

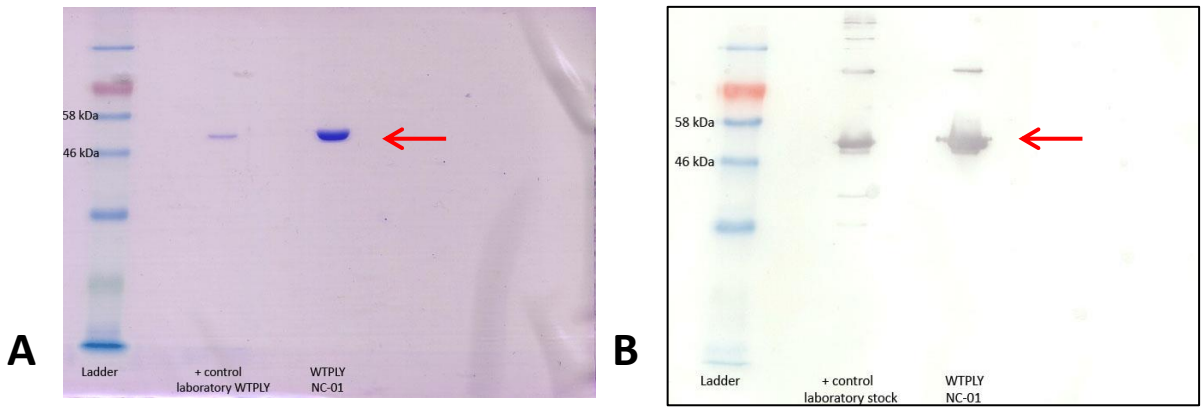

Figure 3.3: Successful purification of wild type pneumolysin batch WTPLY NC-01 A: Coomassie gel for purified WTPLYNC-01. **B:** Western blot for purified WTPLYNC-01. WTPLY NC-01 added at 0.181mg/ml and positive control added at 0.1065mg/ml. Red arrows on Coomassie gel and western blot point to protein of interest, WTPLY at expected molecular weight of 57kDa.

3.1.2 Generation of pneumolysin negative vehicle

A negative vehicle, the solvent of the purified toxin preparation with the His-tagged pneumolysin removed was then generated as described in section 2.1.4 to serve as a negative control in all the cell based assays using the purified toxin. This means that the cells in future experiments will be subjected to anything in the protein preparation except for the pore forming toxin allowing for the distinction between effects that occur due to a possible contaminant such as LPS and PLY itself.

Quality checks for purity and haemolytic activity were performed to determine if the WTPLY was successfully removed. A Coomassie gel and western blot using the neat preparation can be seen in Figure 3.4 labelled as Negative Vehicle. The Coomassie gel did not show any

bands of protein and no band could be seen on the western blot. The concentration of protein in the negative vehicle was then determined by the Nanodrop. The negative vehicle concentration was determined as 0.08mg/ml.

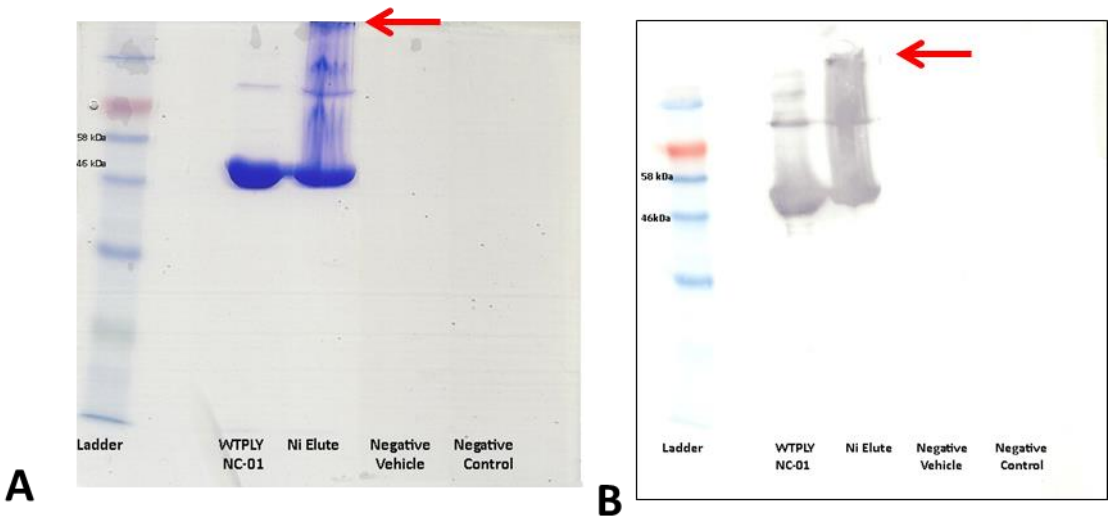

Figure 3.4 Quality **control testing for negative vehicle and nickel elution generated from WTPLY-NC-01 A.** Coomassie gel for WTPLY-NC-01, eluted protein and negative vehicle. **B:** Western blot for WTPLY-NC-01, eluted protein and negative vehicle. Purified wild type pneumolysin (WTPLY-NC), Pneumolysin eluted from magnetic nickel beads (Ni Elute), Negative vehicle created using nickel beads (Negative Vehicle) and dH_2O negative control (Negative Control). All protein loaded at the original purified concentration. Red arrow points to a high molecular weight band found only in the eluted protein.

To recover the protein, magnetic nickel beads are used to bind the His-tag on the recombinant pneumolysin. The protein is eluted off using the same nickel affinity chromatography elution buffer used during the original protein purification. In theory, the imidazole eluted PLY should be fully functional and approximately the same concentration as the WTPLY used to make the negative vehicle. The purpose behind eluting the PLY protein is so it could be added to cell based assays to show that the PLY is unaffected by the process of generating a negative vehicle. The western blot for the eluted protein can be seen in Figure 3.4, labelled as Ni Elute. The eluted PLY has a similar Coomassie profile to WTPLY NC-01.

However, western blot profile showed high molecular weight band that was absent from WTPLY NC-01 [Figure 3.4 Red arrow].

3.1.3 Haemolytic assays to test the functionality of purified, recombinant PLY

Haemolytic assays were then performed on PLY, the negative vehicle and the eluted PLY as described in section 2.2.1. These assays are to test if PLY is functional as a pore forming toxin. Figure 3.5 A shows an image of the haemolytic assay performed on the purified PLY, its vehicle and the elute PLY. This assay has both a qualitative result, as seen by the pellets within the 96 well plate, and a quantitative result, which is determined by first centrifuging the 96 well plate, then collecting the supernatant from the top of each well and reading the absorbance in a plate reader. Where little or no lysis of the red blood cells occurs a small red pellet can be seen in the well. Where lysis does occur, such as when PLY is fully functional there will be no pellet visible. A standard control of pneumolysin (marked as WTPLY CD in the haemolytic assay below) was always used when testing the haemolytic functionality of a newly purified batch of PLY. The WTPLY toxins were added at an approximate 1 in 1000 dilution for a final concentration of 1μg/ml before adding to the PBS to create the necessary dilutions. Both the control and newly purified WTPLY preparations were found to have similar haemolytic ability (Figure 3.5 A). The negative vehicle, which is added without dilution into the assay, closely resembles the negative control of DPBS (Figure 3.5 A).

The endpoint, representing 50% lysis, is the well in the haemolytic assay which has approximately half a pellet of erythrocytes. WTPLY NC-01 and the lab stock pneumolysin both reached 50% lysis in well 5 (Figure 3.5 A). This gives a specific activity of 6.4×10^5 HU/mg for both WTPLY preparations tested.

A second haemolytic assay was performed using DPBS as a negative control and WTPLY NC-01 as a positive control to test the WTPLY eluted from the nickel magnetic

beads (Figure 3.5 B). The eluted WTPLY added at 1µg/ml was found to have no haemolytic activity. The lack of functionality would have to be further investigated as there is no clear reason as to why this occurred

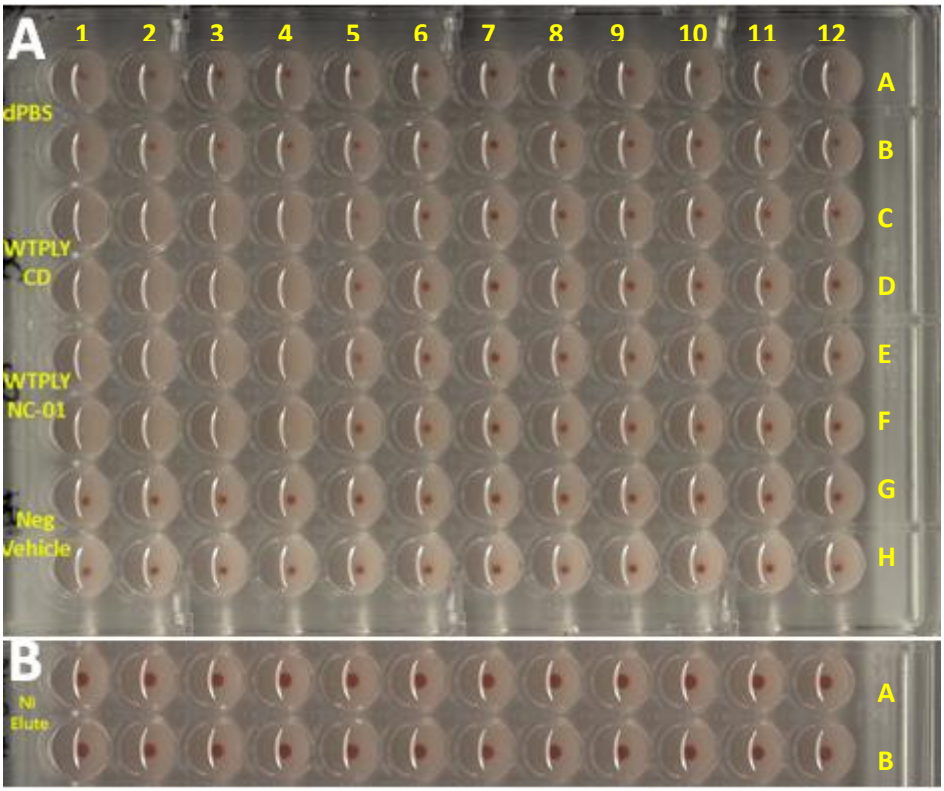

Figure 3.5: Haemolytic analysis of WTPLY NC-01, negative vehicle and nickel elution **A**: Negative control (dPBS), positive control purified wild type pneumolysin from lab stock (WTPLY CD), purified wild type pneumolysin (WTPLY NC-01) and negative vehicle from nickel beads (Neg Vehicle). **B**: Pneumolysin protein eluted from magnetic nickel beads (Ni Elute)

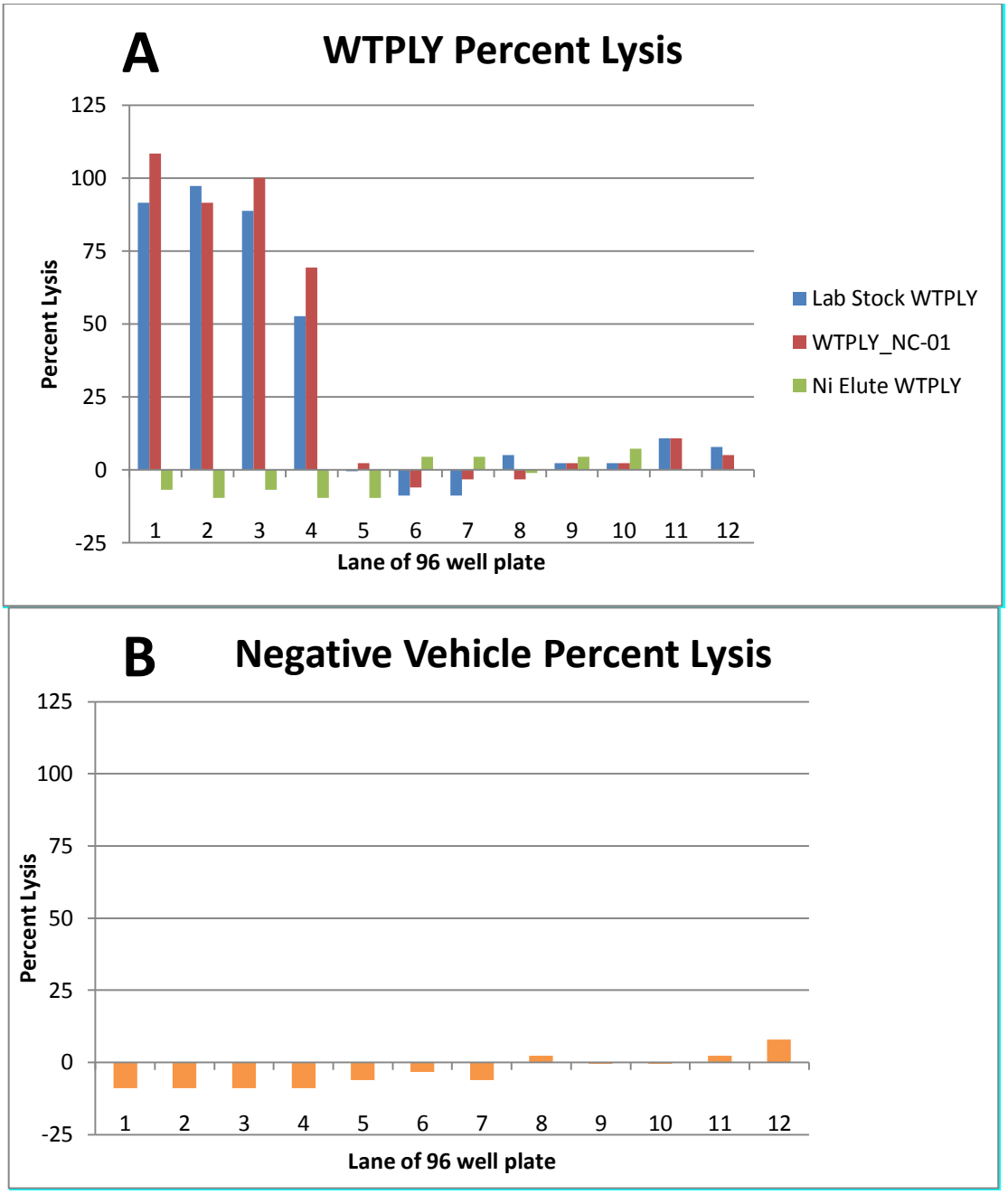

Figure 3.6 Haemolytic proficiency of WTPLY NC-01, nickel elute and negative vehicle. **A:** Graph of percent lysis of erythrocytes by the WTPLY proteins. Concentration of toxin added was 0.25 µg/ml in lane 1 and was serially diluted across the 12 wells. The concentration is halved in each subsequent dilution. **B:** Graph of percent lysis of erythrocytes by Negative Vehicle 100% lysis set to absorbance of lysis caused by highest concentration of lab stock WTPLY at a concentration of 0.00025 mg/ml. Background lysis set to average absorbance of DPBS controls. Concentration of negative vehicle added was 0.08 mg/ml in lane 1 and was serially diluted across the 12 wells. The concentration is halved in each subsequent dilution. No error bars shown as n=1 for this experiment.

To quantitatively compare the haemolytic property of the WTPLY proteins, the percent lysis was calculated and graphed as shown in Figure 3.6 A. The values for the three WTPLY proteins were compared on the same graph as the concentrations used in the haemolytic assay were the same. The percent lysis of erythrocytes in positive control WTPLY (WTPLY CD) was similar in value compared to the purified WTPLY NC-01. In contrast, the WTPLY which was eluted from the nickel beads caused almost no lysis. In fact, when measured against the background of DPBS some of the percent lysis values for eluted PLY preparation are negative. The negative vehicle percent lysis was plotted on a separate graph as this preparation was added to the haemolytic assay undiluted resulting in different concentrations. The percent lysis for the negative vehicle can be seen in Figure 3.6 B. As expected from the qualitative results of the haemolytic assay the negative vehicle showed no lysis when compared to the background negative control of DPBS.

3.1.4 Purification of Δ6PLY

The protein Δ6PLY was generated as described in Kirkham et al. (2006), by inducing a double amino acid deletion of the alanine at position 146 and the arginine at position 147 using a site directed mutagenesis kit (Kirkham, 2006). The deletion of these amino acids in Δ6PLY results in a loss of the haemolytic ability seen in WTPLY.

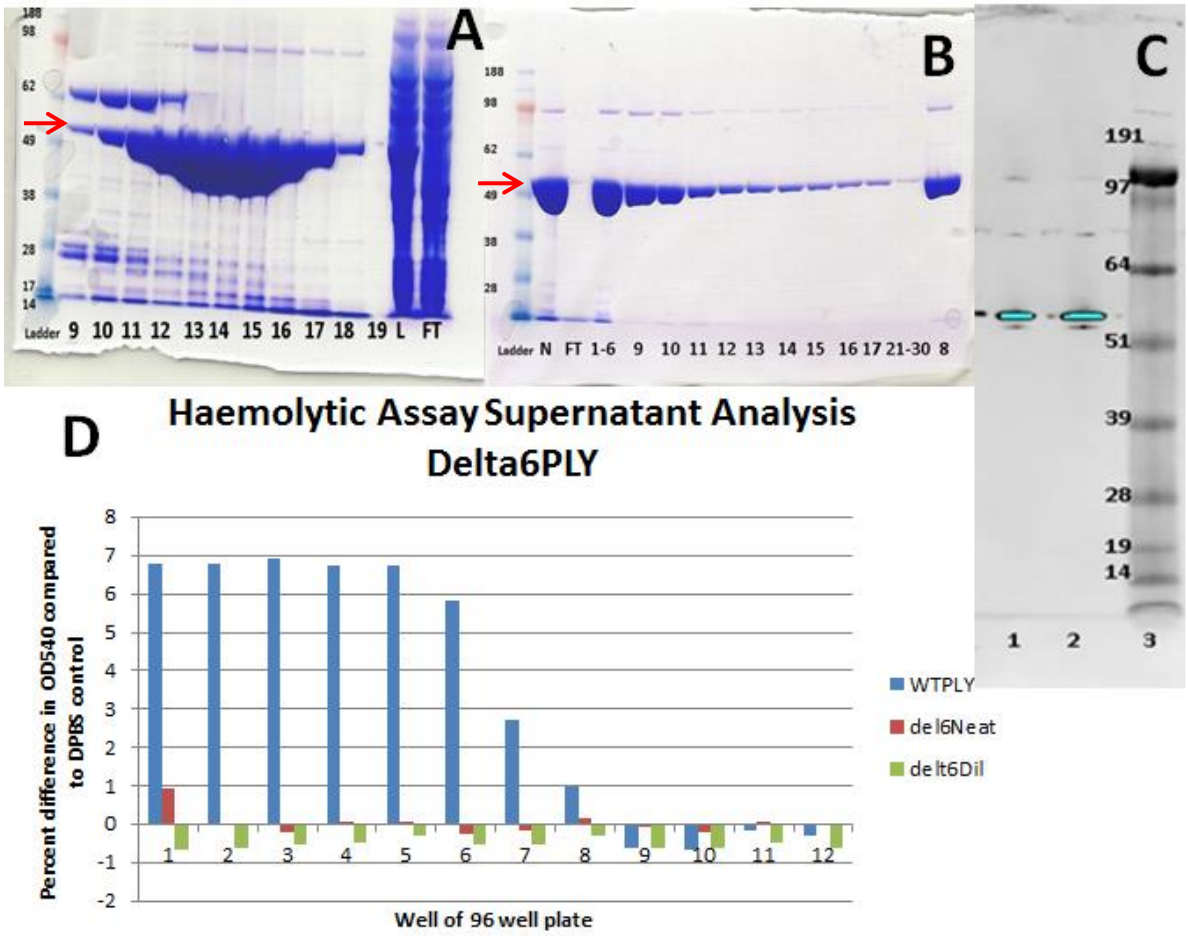

Figure 3.7: Successful purification of Δ6PLY A) Coomassie gel depicting chosen fractions eluted from the NAC column. Red arrow indicates protein of interest **B)** Coomassie gel depicting chosen fractions eluted from the AEC column Red arrow indicates protein of interest **C)** Western blot using anti-PLY rabbit polyclonal antibody and Odyssey visualization with anti-rabbit 800 secondary. Lane assignments **1)** 1.81µg/ml WTPLY **2)** 1.17µg/ml Δ6PLY **3)** SeeBlue2 protein ladder **D)** Graph of haemolytic assay supernatant absorbencies compared to DPBS control supernatant

As with WTPLY, nickel affinity chromatography was chosen to extract the protein as Δ6PLY also has an incorporated his-tag. This again was followed by anion exchange chromatography which was used to purify out contaminants, such as LPS. The protein concentration was read by small volume spectrophotometer, Nanodrop. Quality control checks were performed as in WTPLY to verify purity and determine haemolytic properties.

3.1.5 Δ6eGFPPLY

The protein Δ6eGFPPLY was generated as described in the PhD thesis of Dr. Graeme Cowan (Cowan, 2006). An enhanced green fluorescence protein (eGFP) gene was cloned into the already established pET33b vector expressing Δ6PLY created by Kirkham et al. (2006) to fuse the GFP protein to the N terminal end of Δ6PLY. This was to avoid the large fluorescent molecule interfering with the binding of the protein that occurs via domain 4 on the C-terminal end of the protein.

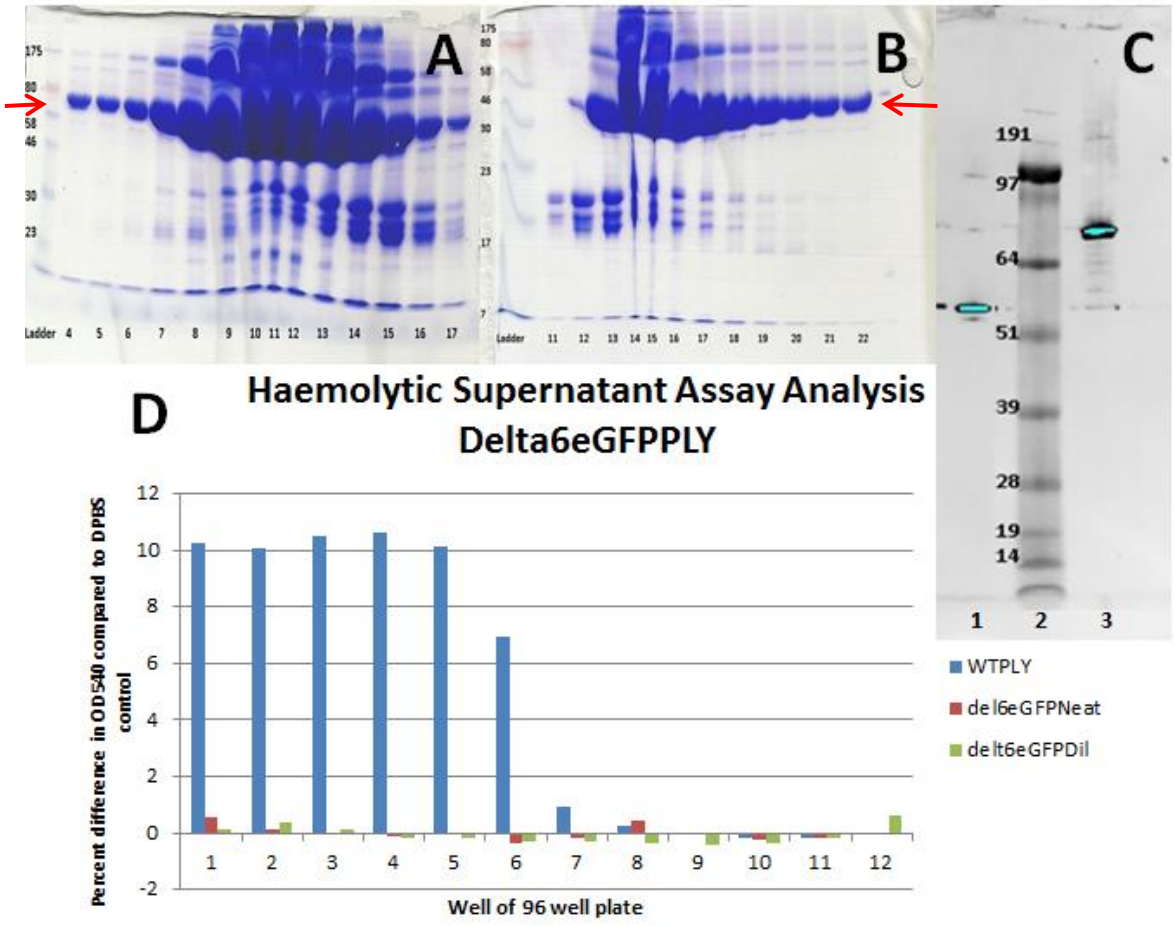

Figure 3.8: Successful purification of Δ6eGFPPLY A) Coomassie gel depicting chosen fractions eluted from the NAC column. Red arrow indicates protein of interest **B)** Coomassie gel depicting chosen fractions eluted from the AEC column. Red arrow indicates protein of interest. **C)** Western blot using anti-PLY rabbit polyclonal antibody and Odyssey visualization with anti-rabbit 800 secondary. Lane assignments **1)** 1.81µg/ml WTPLY **2)** SeeBlue2 protein ladder **3)** 1.12µg/ml Δ6eGFPPLY **D)** Graph of haemolytic assay supernatant absorbencies compared to DPBS control supernatant

The Δ6eGFPPLY protein purification was completed using nickel affinity chromatography to extract the protein as it has an incorporated his-tag and anion exchange chromatography to purify out contaminants has an incorporated his-tag its purification, such as lipopolysaccharide (LPS). The protein concentration was determined by Nanodrop and used in various quality control assays including a haemolytic assay to ensure it does not have haemolytic properties and a Western blot to visualize purity (Figure 3.8).

3.2 Cell Based Assays

3.2.1 LDH and MTT assays in L929 fibroblast cells

In order to identify sublytic concentrations of WTPLY for use in further experiments, cell based assays using fibroblasts were used. These cells were used as they are easy to grow and were previously used by the research group so the results could be compared between batches of toxin. The assays using these cells will serve not only as a quality control but also as a guide for what concentrations of WTPLY NC-01 cause cell death above 5%. Lactate dehydrogenase (LDH) assays are one type of assay used. LDH assays are used to determine cytotoxicity of cells by analysing the levels of the LDH enzyme, an enzyme normally found in the cytoplasm which is released from the cell into the supernatant upon cell lysis (described in 2.2.2). However, in the case of large pore forming toxins such as pneumolysin, the LDH assay determines cell permeability as the pores created are large enough to allow the LDH enzyme to exit without complete cell lysis. Another type of assay used, MTT assays, are cell viability assays. MTT assays measure formazan, an insoluble purple compound, which is the product of the conversion of MTT by cell mitochondria. This conversion process to formazan can only proceed when the cell is alive and if a cell is dead the MTT compound remains its original yellow colour (described in 2.2.3).

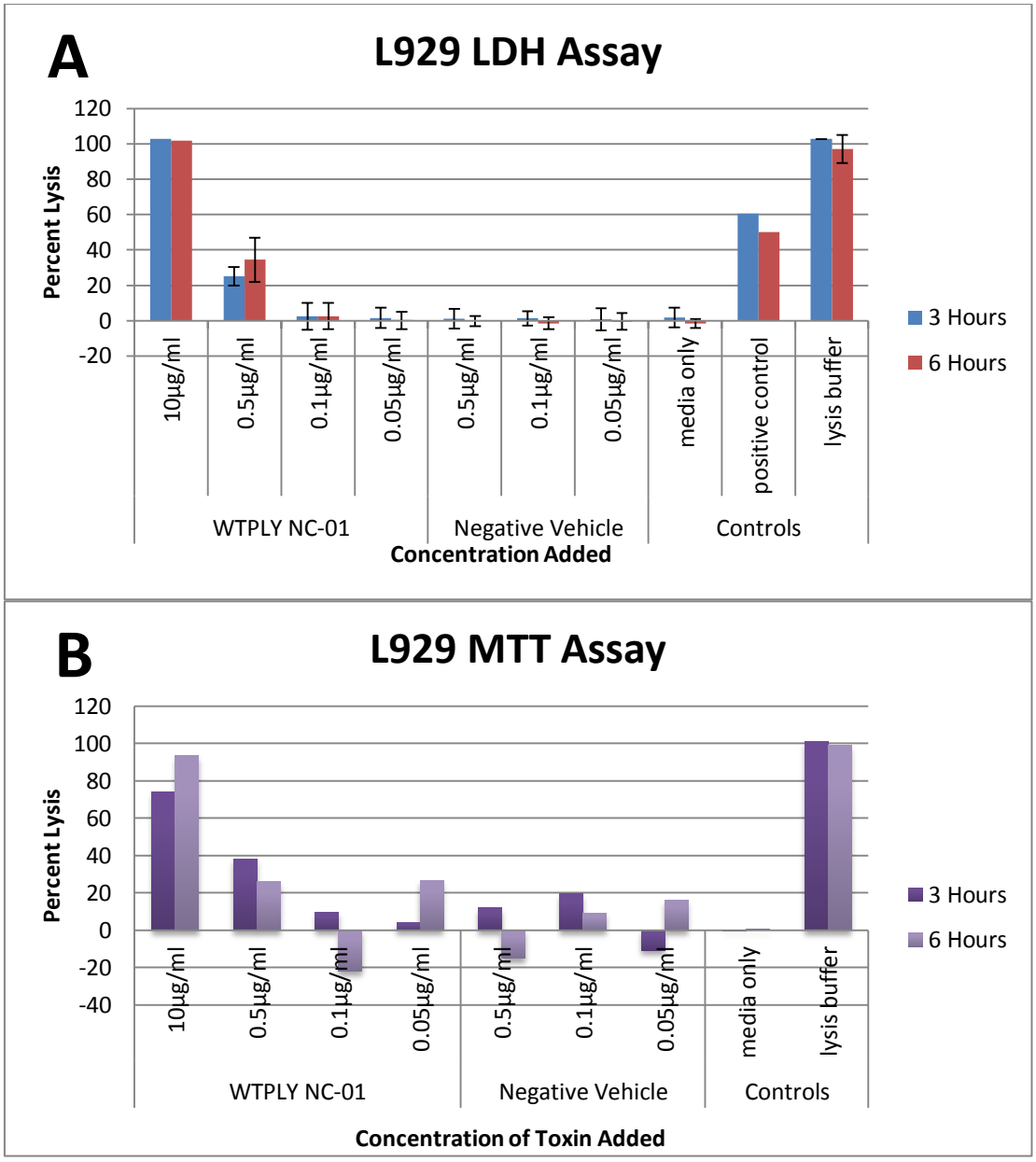

Figure 3.9 Results of varying pneumolysin concentrations on the membrane permeability and viability of L929 fibroblast cells A) LDH Assay for L929 fibroblast cells exposed to toxin or negative vehicle for either 3 or 6 hours. Lysis buffer was used as 100% lysis and media only negative control was used as background to determine percent lysis. Positive control described as, bovine heart LDH, was issued by the manufacturer to ensure performance of the kit. Error bars indicate standard deviation between experiments as n=2. **B)** MTT Assay for L929 fibroblast cells exposed to toxin or negative vehicle for 3 or 6 hours. Lysis buffer set the value for 100% cell death. Media only wells used as one of the negative controls provided the value for background. The results shown are from a single replicate, n=1.

The graphical results for both the LDH and MTT are similar. A concentration of 10µg/ml of WTPLY NC-01 resulted in 100% cell lysis in the LDH assay and in the MTT

assay resulted in 75% cell death by 3 hours and 93.5% cell death by 6 hours. At 0.5µg/ml the percent of dead and lysed cells decreased to less than half the cells tested. At 0.1µg/ml, the expected sublytic concentration as recorded in literature, a low percent of cell lysis, 7.44%, was seen even after 6 hours of exposure to the toxin. The negative vehicle (preparation described in 2.1.4) had a maximum cell lysis of 2.55% after 6 hours at 0.05µg/ml and a maximum cell death of 19.5% at a concentration of 0.1µg/ml after 3 hours exposure in L929 cells.

3.2.2 LDH assays in A549 lung epithelial cells

Lactate dehydrogenase (LDH) assays were used to determine the cytotoxicity that occurs in A549 lung epithelial cells when exposed to different concentrations of wild type pneumolysin in order to determine sublytic concentrations of the toxin. This colorimetric assay detects the LDH enzyme, which is usually found in the cell cytoplasm but releases into the supernatant when the cell undergoes lysis. The full method used is detailed in Section 2.2.2.

A549 cells were exposed to the wild type toxin or a negative vehicle for 3 or 6 before the supernatant was removed. The supernatants were then analysed by plate reader and the percent lysis was determined. The lysis buffer supplied by the manufacturer was used to set the 100% lysis value and the media only control was used to set the background absorbance value. Sublytic concentrations are defined as less than 5% cell lysis. According to the results, the pneumolysin concentration with a percent lysis that fit the sublytic criteria was a concentration of 0.1µg/ml or 1.8µM. The negative vehicle which served as the negative control recorded percent lysis in the negative figures for most of concentrations tested indicating that no cytotoxicity occurred in these cells for the time exposed.

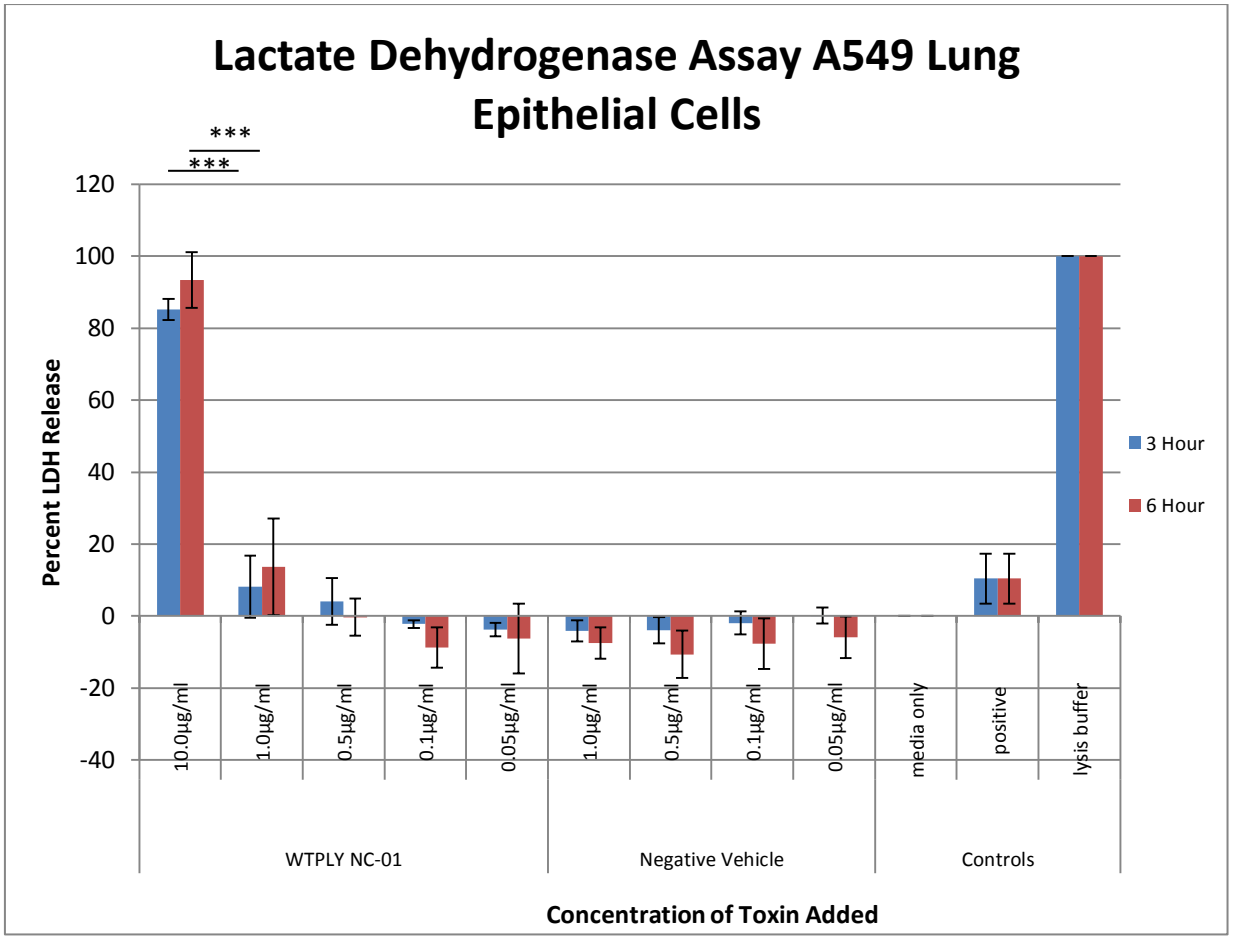

Figure 3.10:Effect of WTPLY NC-01 on the Membrane Permeability of A549 Lung Epithelial Cells. A549 lung epithelial cells were exposed to wild type pneumolysin toxin or negative vehicle for 3 or 6 hours before the supernatant was removed for analysis. Lysis buffer was used as 100% lysis and media only negative control was used as background to determine percent lysis. Positive control described as, bovine heart LDH, was issued by the manufacturer to ensure performance of the kit. Error bars indicate standard deviation between experiments as n=3. Statistical signficance indicated by *** ($p<0.005$).

3.3 Determining sublytic pneumolysin concentrations in A549 lung epithelial cells

3.3.1 Confocal microscopy using eGFPPLY

While cell based assays provide a quantitative measurement for the damage wild type PLY was doing to A549 lung epithelial cells, confocal microscopy was used to provide qualitative analysis. Wild type PLY labelled with eGFP (eGFPPLY) was utilized as described in section 2.4.1 so that both cell morphology and toxin localization could be seen. The sublytic concentration for WTPLY is 1.8µM as found by LDH assay in section 3.2.2 above.

At a concentration of 1.1µM of eGFPPLY [Figure 3.11 A and B] the A549 cells were adhered to the slide with no obvious membrane blebbing or rounding both of which are markers of apoptosis. When the concentration of eGFPPLY was increased 10 times to 11.1µM of eGFPPLY [Figure 3.11 C and D] some of the cells began to show evidence of apoptosis and cell lysis. Figure 3.10 LDH assay results support this as there is a rise in LDH release when PLY is at 1.0µg/ml over the sublytic concentration of 0.1µg/ml. The majority of cells exhibited membrane blebbing and their morphology appeared rounded as the cells began detaching from the slide. Although in the minority, there were a few cells that still appeared normal and undamaged at this concentration. At the 111.5µM [Figure 3.11 E and F] concentration of eGFPPLY most of the cells were rounded and dead. Some evidence of nuclear disruption can be seen as indicated by a decrease in the DAPI staining shown in blue. The remaining cells were in the process of apoptosis as evident by extensive membrane blebbing.

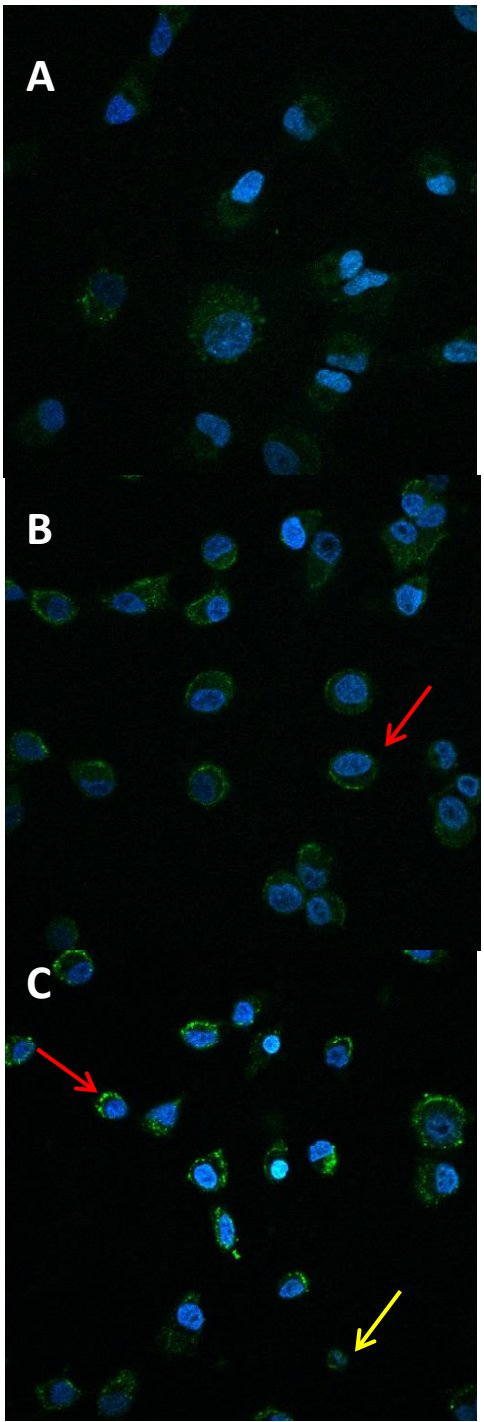

Figure 3.11: Effects of eGFPPLY toxin on A549 lung epithelial cells. A eGFPPLY added at a concentration of 1.1µM **B)** eGFPPLY added at a concentration of 11.1µM. **C)** eGFPPLY added at a concentration of 111.5µM. In all conditions toxin was added and cells were incubated for 30 minutes at 37^{o}C and 5% CO_2 before fixation. Red arrows indicate cells with evidence of membrane blebbing and yellow arrows indicate cells with evidence of cell rounding. Images were taken via confocal microscopy at 60x magnification under oil immersion. Blue staining corresponds to nuclei stained by DAPI and green staining corresponds to eGFP conjugated pneumolysin toxin.

3.4 Effects of PLY and Δ6PLY toxoid in A549 lung epithelial cells

3.4.1 Live cell microscopy using Δ6eGFPPLY

To determine whether the Δ6eGFPPLY toxin would have any adverse effects on the A549 lung epithelial cells that would cause variation in using it as a non-haemolytic control, a simple experiment in which monolayers of A549 cells were exposed to the toxin 30 minutes before visualisation without a fixation step was performed [Figure 3.12]. Although the lack of cytotoxicity of Δ6eGFPPLY was previously demonstrated for another cell type, L929 fibroblast cells in the study by Kirkham et al (2006) but this experiment was performed to ensure relevance for this project's cell type of interest.

All images were taken at 20x and 40x magnification as oil immersion cannot be used in conjunction with live cell imaging which caused difficulty in seeing the exact localisation of the toxin on the cells. The low magnification also proved difficult as there was a lack of fluorescence signal from some of the lower concentrations of toxin causing the image to look faint [Figure 3.12]. What was obvious was that even at concentrations 100x greater than that of a lethal dose of WTPLY [Figure 3.12], the Δ6eGFPPPLY toxin did very little to effect the morphology of the A549 cells indicating its lack of cytotoxic effects[Figure 3.12 H-J].

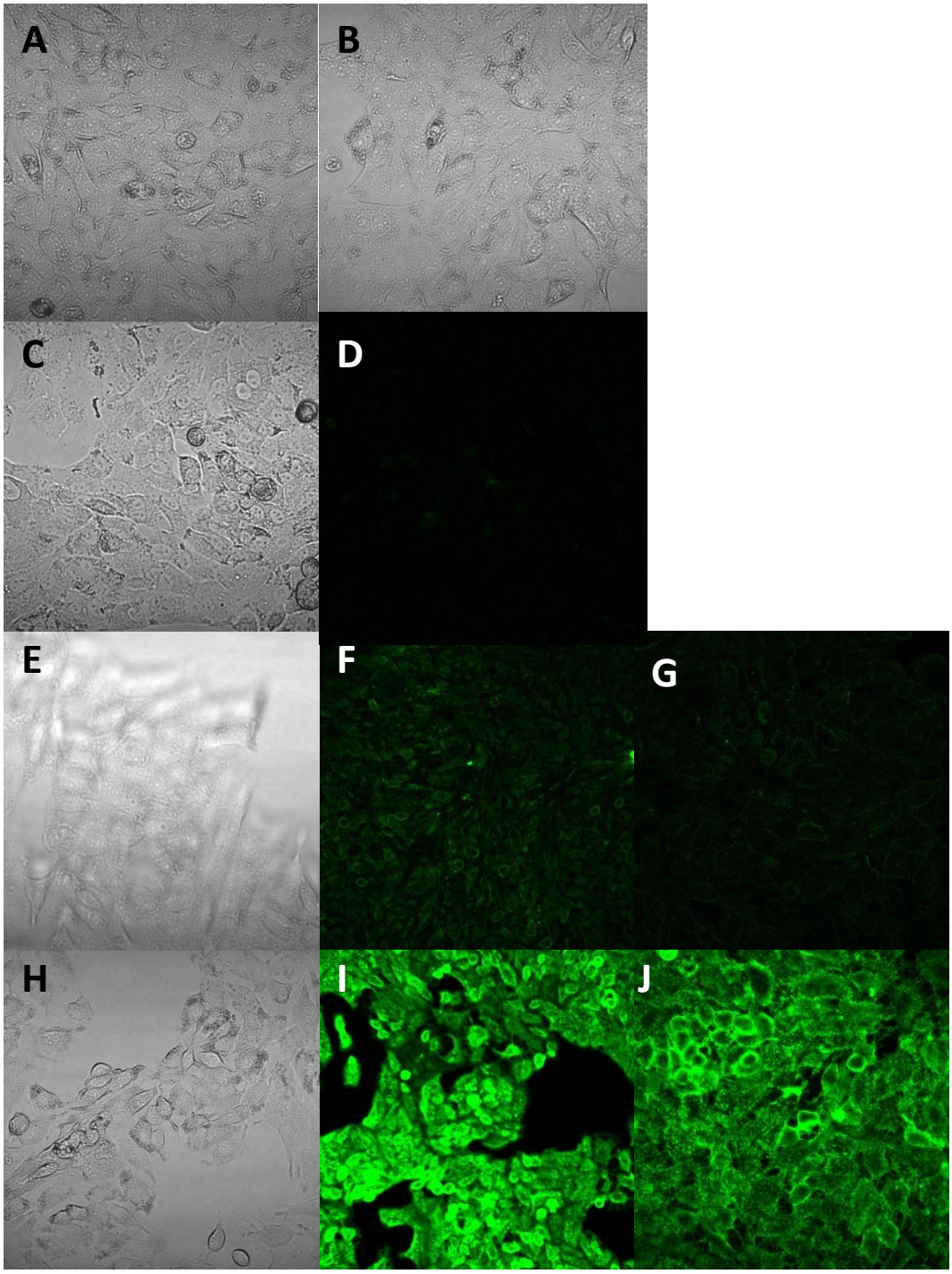

Figure 3.12: Live cell fluorescence imaging of the effects of Δ6eGFPPLY toxin on A549 Lung Epithelial Cells. A549 cells were grown to a monolayer in a 24 well plate before being exposed to varying concentrations of Δ6eGFPPLY for 30 minutes. The cells were washed and colourless RPMI was added before immediately being visualised by fluorescence microscopy at 20x or 40x magnification. **A)** Bright field image of control cells not exposed to Δ6eGFPPLY at 40x magnification **B)** Bright field image of A549 cells exposed 1.8µM of Δ6eGFPPLY at 40x magnification. **C-D:** A549 cells exposed to 18.1µM of Δ6eGFPPLY **C)** Bright field image at 40x magnification. **D)** Fluorescence image at 20x magnification. **E-G:** A549 cells exposed to 180.6µM of Δ6eGFPPLY **E)** Bright field image at 40x magnification. **F)** Fluorescence image at 20x magnification. **G)** Fluorescence image at 40x magnification. **H-J:** A549 cells exposed to 1.8mM of Δ6eGFPPLY **H)** Bright field image at 40x magnification. **I)** Fluorescence image at 20x magnification. **J)** Fluorescence image at 40x magnification.

3.4.2 Immunostaining of F-actin, E-cadherin and eGFP labelled toxin in A549 cells

To investigate the possible roles of E-cadherin and actin in invasion, preliminary immunofluorescence was performed by staining A549 cell monolayers with E-cadherin and actin antibodies in absence of any toxin. This allowed for the optimization of the microscopy staining protocol before the addition of any experimental elements.

As described in the Methods and Materials [section 2.5.1], A549 cell monolayers were fixed, permeabilized and stained with E-cadherin to visualize cell-cell contacts. The results are shown in the representative image in Figure 3.13. It should be highlighted that even at very high primary and secondary concentrations of antibody, as well as high gain set on the microscopy software, the E-cadherin fluorescent signal was very low and cell to cell contacts were barely visible. The staining was also inconsistent across the monolayer.

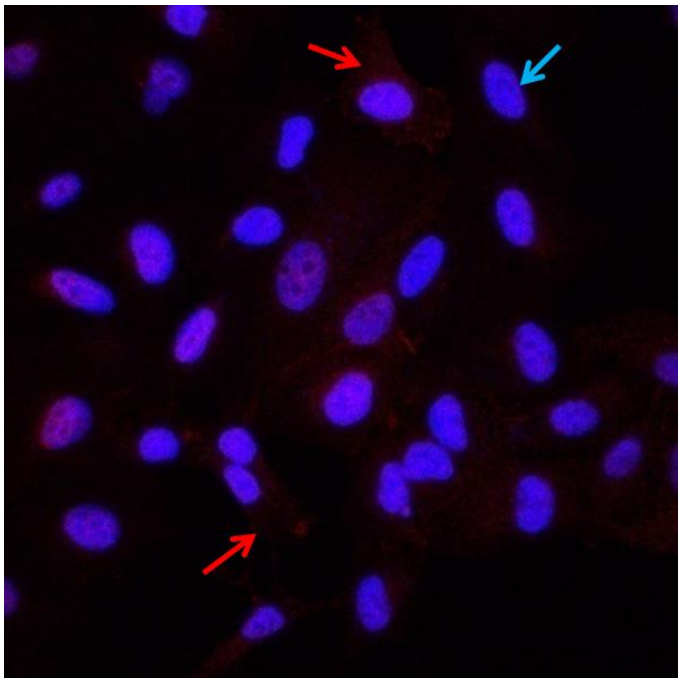

Figure 3.13: E-cadherin immunostaining of A549 cells. A549 lung epithelial cells were grown to a monolayer on a coverslip before being fixed and stained with 1 in 50 dilution of E-cadherin primary antibody and 1 in 500 dilution of Alexa Fluor 633 secondary antibody. Coverslip was imaged by confocal microscopy at 60x magnification using oil immersion. Blue staining corresponds to nuclei stained by DAPI (example marked by blue arrow) and red staining corresponds to E-cadherin immunostaining (examples marked by red arrows).

After the initial E-cadherin immunofluorescence experiments, the second component of the triplex immunostaining, F-actin, was tried to test the staining potential of the immunofluorescence protocols. To accomplish this, a fluorescence conjugated phallodin antibody was utilized [Materials and Methods 2.5.2]. Figure 3.14A depicts the results of

staining A549 monolayers for F-actin fibres which were clearly seen in all of the cells. A bright field image was used as a control to visualize the cell morphology and can be seen in Figure 3.14B. The bright field images show the A549 cells had no obvious morphological abnormalities as a result of the immunofluorescence protocol.

After confirmation of the immunofluorescence protocol by actin staining, toxin exposure was combined with the F-actin staining to try to optimize a dual staining technique and get an idea of the possible localisation of PLY and Δ6PLY toxin in respect to A549 cells. A control of toxin exposure without actin staining was performed using 2.2µM of eGFPPLY which was applied throughout this experiment to discern if any evidence of cytotoxicity to the cells could be seen [Figure 3.14 C and D]. The higher concentrations of eGFPPLY, 11.1µM and 111.5µM [Figure 3.11 D and F], have obvious cytotoxic effects, while, the bright field image of cells exposed to 2.2µM of eGFPPLY [Figure 3.14 D] showed no evidence of apoptotic effects such as rounding or membrane blebbing.

A sublytic concentration of 2.2µM of eGFPPLY and 2.2µM of Δ6eGFPPLY, A549 cells were exposed to the respective toxin before fixation, permeabilization and staining for F-actin. The microscopy images of the experiments using these two toxins are as shown in Figure 3.14 E-F for cells exposed to eGFPPLY and Figure 3.14 G-H for cells exposed to Δ6eGFPPLY. The F-actin staining seems to be brighter in the case of the non-haemolytic Δ6eGFPPLY exposure compared with the conjugated wild type toxin, eGFPPLY. The images show the majority of the eGFP staining is located near the nucleus of the cells for both the conjugated wild type toxin and the non-haemolytic variant [Figure 3.14 E and G marked by yellow arrows]. The eGFPPLY exposed cells appearing to have a greater amount of toxin staining. Both bright field images prove the A549 cells themselves had no adverse effects due to toxin exposure as the cell morphology of the monolayers appeared normal [Figure 3.14 F and H].

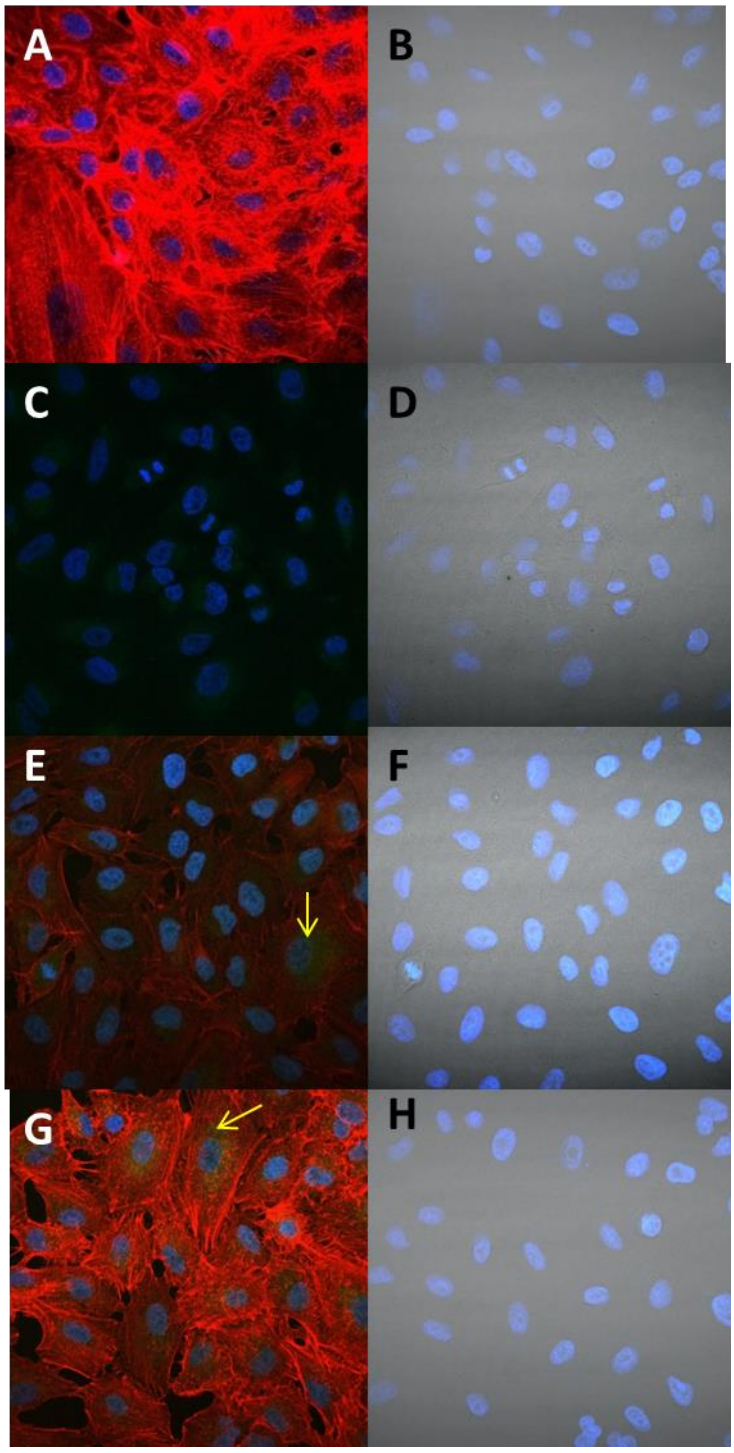

Figure 3.14: Immunofluorescence staining of F-actin after exposure of A549 cells to either eGFPPLY or Δ6eGFPPLY. A549 lung epithelial cells were grown to a monolayer on a coverslip before the appropriate samples were exposed to the corresponding toxin for 30 minutes at 37°C and 5% CO_2. Cells were then fixed and were appropriate stained with 1 in 500 dilution of Alexa Fluor Phalloidin 555 antibody to detect F-actin. **A-B)** Control slide for F-actin staining of A549 without exposure to toxin. Images were taken in confocal fluorescence and bright field. **C-D)** Control slide for 2.2µM eGFPPLY toxin exposure without F-actin staining. Images were taken in confocal fluorescence and bright field. **E-F)** Slide with A549 cells exposed to 0.2µg/ml eGFPPLY then fixed and stained for F-actin. Images were taken in confocal fluorescence and bright field. **G-H)** Slide with A549 cells exposed to 2.2µM Δ6eGFPPLY then fixed and stained for F-actin. Images were taken in confocal fluorescence and bright field. Coverslip was imaged by confocal microscopy at 60x magnification using oil immersion. Blue staining corresponds to nuclei stained by DAPI, green staining corresponds to eGFP conjugated toxin (examples marked with yellow arrows) and red staining corresponds to actin immunostaining.

The A549 cells visualized under 60x magnification showed no obvious signs of colocalization of PLY toxin with actin fibres. This may be due to the use of a lower resolution in this experiment than used in the study by Hupp et al. 2012 which found colocalization of

PLY with actin (Hupp, 2012). The lower resolution led to the toxin particles not being distinct enough to really see where they are attached but instead show as green specks dispersed amongst the cell.

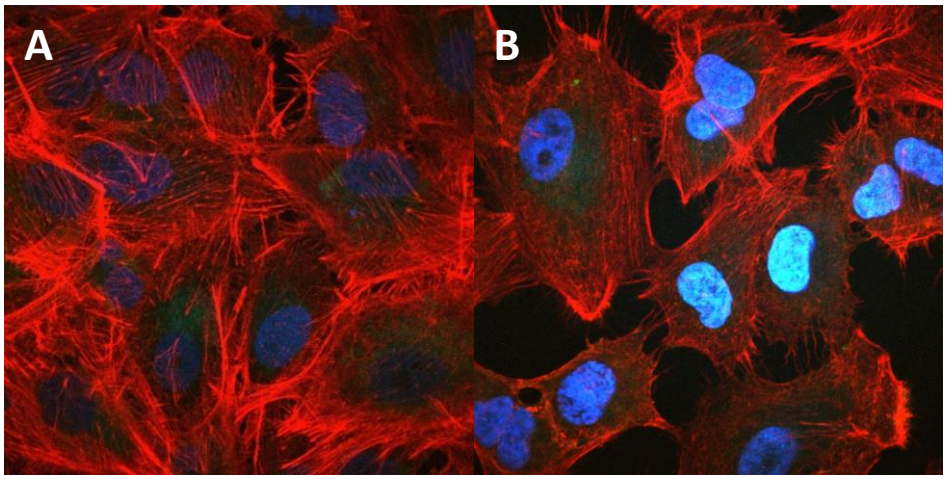

Figure 3.15: High magnification of F-actin staining after A549 exposure to either eGFPPLY or Δ6eGFPPLY. A549 lung epithelial cells were grown to a monolayer on a coverslip before being exposed to the corresponding toxin for 30 minutes at 37^{o}C and 5% CO_2. Cells were then fixed and stained with 1 in 500 dilution of Alexa Fluor Phalloidin 555 antibody to detect F-actin. **A)** Slide with A549 cells exposed to 3.3µM eGFPPLY then fixed and stained for F-actin. Images were taken in confocal fluorescence and bright field. **B)** Slide with A549 cells exposed to 11.1µM Δ6eGFPPLY then fixed and stained for F-actin. Images were taken in confocal fluorescence and bright field. Coverslip was imaged by confocal microscopy at 100x magnification using oil immersion. Blue staining corresponds to nuclei stained by DAPI, green staining corresponds to eGFP conjugated toxin and red staining corresponds to actin immunostaining.

In order to visualize using a 100x oil immersion lens, cell monolayers were again grown and exposed to toxin before immunostaining for F-actin. A concentration of 3.3µM eGFPPLY, the maximum that could be used without causing cytotoxicity, was added to A549 lung epithelial cells. The results for the exposure to conjugated wild type toxin are shown in [Figure 3.15A]. The Δ6eGFPPLY was added at a much higher concentration of 11.1µM to the A549 cells as this version of the toxin was not found to cause haemolysis. The concentration was increased with the Δ6eGFPPLY compared to the eGFPPLY to test whether more distinct, bright toxin aggregations could be seen. The results are depicted in Figure 3.15 B. Neither

toxin exposures even at 100x magnification resulted in the distinct colocalization seen in the Iliev research group paper (Hupp, 2012).

3.4.3 Western blotting for E-cadherin and actin in A549 whole cell lysates

Due to the weak E-cadherin immunofluorescence staining, it was decided to test for E-cadherin protein levels in A549 whole cell lysates to determine if adequate levels of the protein existed in the monolayers being stained for microscopy. Section 2.6 in the Materials and Methods details the process for Western blotting followed. Figure 3.19 shows the results of a Western blot run using protein from A549 whole cell lysates and probed for E-cadherin and actin. Actin was used a loading control in the experiment to ensure that any change in E-cadherin seen were not just due to more protein being added. By utilizing two different secondary conjugated proteins and the Licor Odyssey Infrared Imaging system, both actin and E-cadherin can be seen on the same membrane allowing for direct comparison. E-cadherin was labelled with a secondary antibody specific for mouse immunoglobins which could be visualized in the 800nm, green channel. Actin, which served as a control, was labelled with a secondary antibody specific for rabbit immunoglobins which could be visualized in the 700nm, red channel. The specific secondary antibodies allow for the protein of interest and control to be probed on the same membrane for greater accuracy of any deviations in the loading control.

The actin, loading control bands could be seen albeit in differing concentrations in every lysate loaded in red colour highlighted by the pink boxes at an approximate molecular weight of 42kDa [Figure 3.16]. E-cadherin bands, highlighted by the yellow boxes, were faint but could be seen at the approximate molecular weight of 100kDa in the sublytic, 0.1µg/ml pneumolysin treated cell lysates and the whole cell lysate controls made from A549 monolayers [Figure 3.16]. A549 cells exposed to lytic concentrations of pneumolysin,

10µg/ml, were found to have no visible 100kDa band and therefore were found negative to E-cadherin [Figure 3.16].

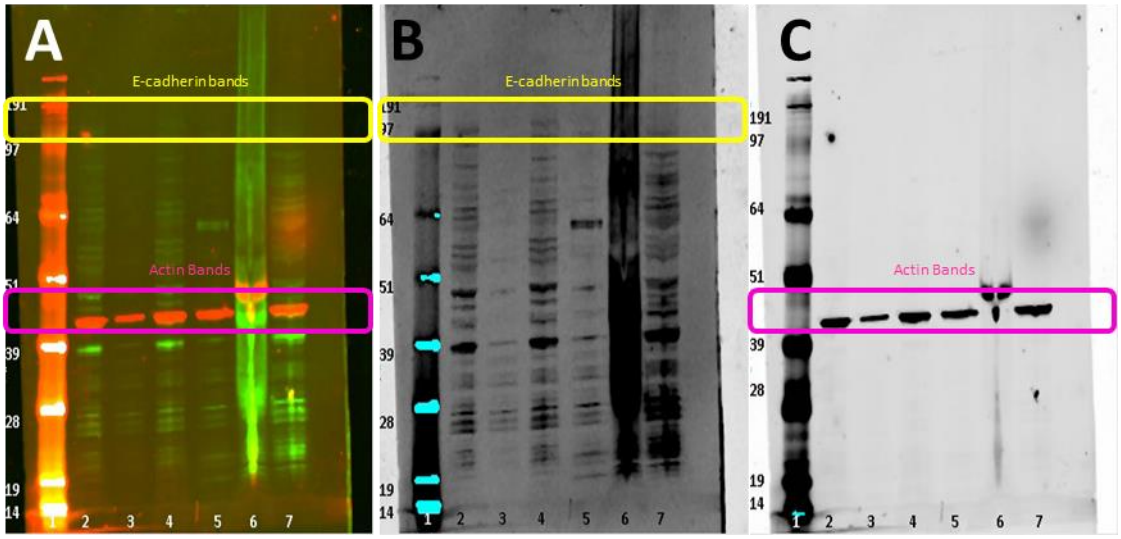

Figure 3.16 Effect of pneumolysin on E-cadherin in A549 whole cell lysates. **A)** Dual channel scan of 700nm and 800nm channels by Licor Odyssey Imager. **B)** Grey scale of 800nm channel only, specific for E-cadherin antibody. **C)** Grey scale of 700nm channel only, specific for actin antibody. Lanes assignments: **1)** SeeBlue2 prestained protein ladder **2)** A549 whole cell lysate by lysis buffer after 1 hour treatment with 0.1µg/ml PLY, supernatant **3)** A549 whole cell lysate by lysis buffer after 1 hour treatment with 10µg/ml PLY, supernatant **4)** A549 whole cell lysate by lysis buffer after 1 hour treatment with 0.1µg/ml PLY, supernatant and cell debris **5)** A549 whole cell lysate by lysis buffer after 1 hour treatment with 10µg/ml PLY, supernatant and cell debris **6)** A549 whole cell lysate by lysis buffer, supernatant **7)** A549 whole cell lysate by lysis buffer, supernatant and cell debris. E-cadherin bands are about 100kDa and are in the 800nm channel so they appear green (highlighted by yellow boxes). Actin loading control bands are about 42kDa and are in the 700nm channel so they appear red (highlighted by pink boxes).

3.4.4 Effect of pneumolysin and polysaccharide capsule on adherence of *S. pneumoniae* to A549 lung epithelial cells

Adherence of *S. pneumoniae* to a host cell is the first stage in the invasion process. To determine the traits in this bacterium that lead to adherence, various strains of *S. pneumoniae* were tested in an adherence assay [Materials and Methods section 2.7] to assess how well each strain adhered to A549 lung epithelial cells, a common cell type encountered by this bacterium.

A graph showing the results of three replicate adherence assays can be found in Figure 3.17. The acapsular strains of *S. pneumoniae* adhered better to the A549 cells than the stains which were surrounded by a polysaccharide capsule. The R6 acapsular, laboratory strain was found to adhere to A549 cells the best with an average percent adherence of 34.992%. Strong statistical significance exists between the adherence achieved by the acapsular R6 and all of the capsular serotype 2 D39 strains.

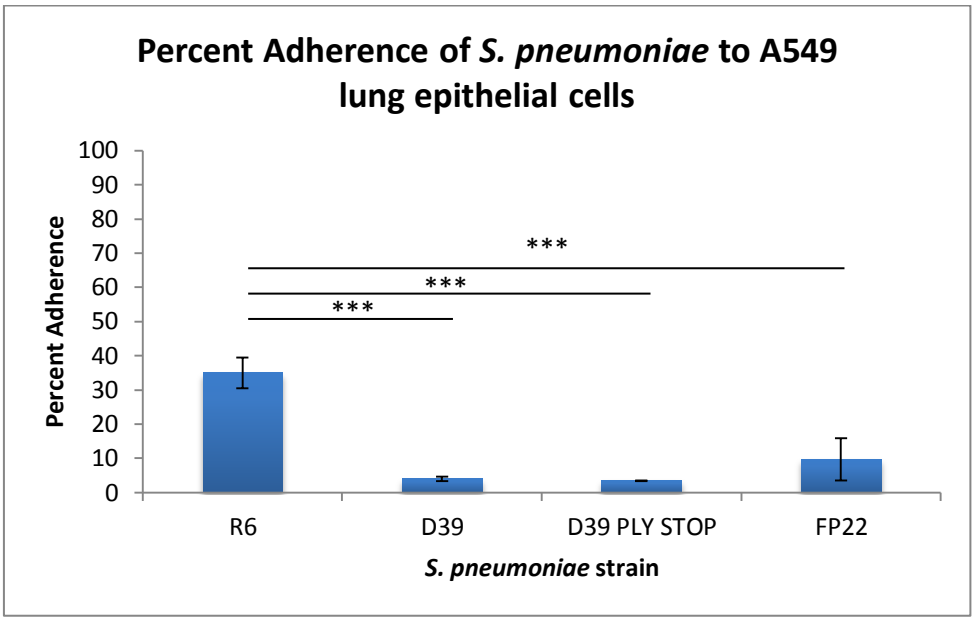

Figure 3.17 Adherence of various *S. pneumoniae* strains to A549 lung epithelial cells. *S. pneumoniae* was added to monolayers of A549 cells at a density of $1x10^7$ bacteria/ml. Percent adherence was calculated by dividing the adhered bacteria recovered after washing the monolayers by the starting inoculum added. All counts were determined by serial dilution, viable counting. D39 = virulent, serotype 2, clinical isolate; D39 PLY STOP = D39 mutant in which the PLY gene has a premature stop codon resulting in a non-functional toxin; D39 FP22 = acaspsualar D39 created by Pearce et al. 2002 by insertion of a kanamycin cassette deleting the capsule locus; R6 = acapsular, avirulent laboratory strain that is a descendent of the serotype 2 clinical isolate, D39 strain. Error bars depict standard deviation between experiments as n=3. Statistical significance depicted by *** ($p<0.005$).

The ability to produce pneumolysin did not appear to affect adherence as no statistical significance was found between the adherence of D39 wild type and the PLY negative mutant D39 PLY STOP strain.

FP22, a knockout strain of D39 that does not produce a capsule, was found to adhere better to A549 cells than either of the capsular strains tested. The average percent adherence of FP22 was 9.693% rather than the 3.932% seen in D39 and 3.503% seen in the D39 PLY STOP strain. However, the difference in adherence between these three strains was not statistically significance.

3.5 Optimisation of the Experiment Environment for Host-Toxin Interactions

3.5.1 Introduction of pJWV25 plasmid into *S. pneumoniae*

The pJWV25 plasmid was created in a study by Eberhardt et al. in 2009. This plasmid contains a zinc inducible promoter, an ampicillin resistance gene, a tetracycline resistance gene and a gene for GFP+, which is a faster folding variant of GFP [Eberhart, 2009]. A plasmid map of pJWV25 is shown in Figure 3.18 A. The GFP+ gene can be linked to the N-terminus of a protein of interest using a flexible linker region. There is a history of difficulty visualizing GFP in *S. pneumoniae.* This may be due to the acidic interior of the bacterium and the organism's preference for a carbon dioxide rich environment. The Eberhardt et al. study showed the enhanced visibility of GFP+ over the commonly used GFP. The study explained how this new plasmid could be utilized in other studies involving *S. pneumoniae.* The pJWV25 plasmid incorporates into the *S. pneumoniae* genome by a double crossover event. The *E. coli* origin of replication and the ampicillin resistance gene are removed when the plasmid completes the double crossover event and successfully inserts into the *S. pneumoniae* genome.

The pJWV25 plasmid was transformed into *S. pneumoniae* as described in section 2.3.4. Screening primers which identify the successful insertion of pJWV25 DNA into the pneumococcal chromosome by yielding a product with an expected size of 420bp were used in a PCR performed on the genomic DNA isolated from the transformants (described in 2.3.5). The gel electrophoresis photo shown in Figure 3.18 B shows the result of the PCR

screen. The results clearly show one band for each of the two transformants tested at the approximate size of the expected PCR product.

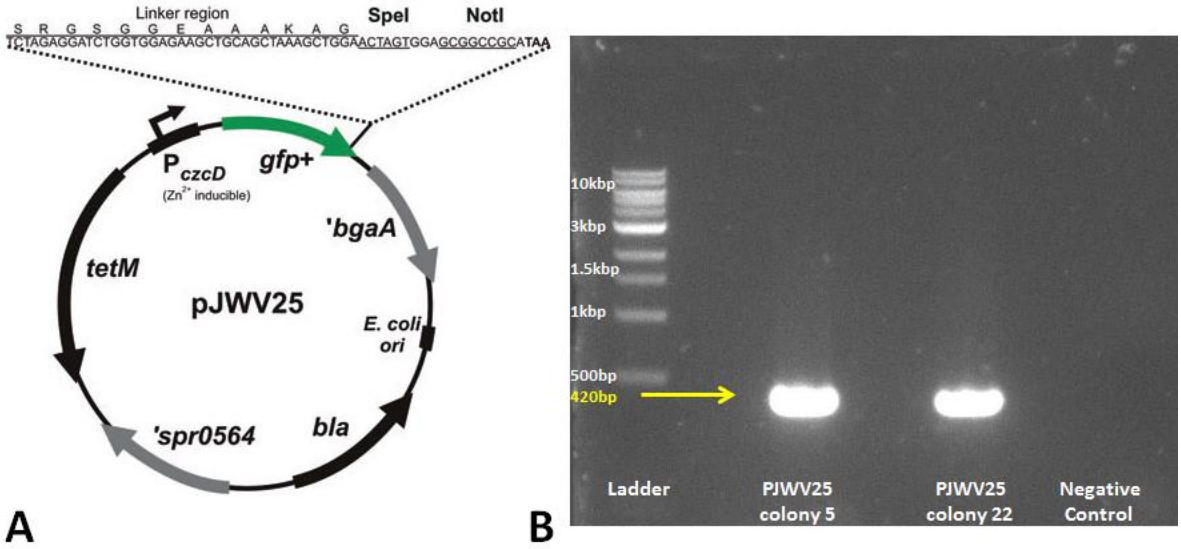

Figure 3.18: Insertion of pJWV25 plasmid into *Streptococcus pneumoniae*. A: Plasmid map of the pJWV25 plasmid from Eberhardt et al. 2009. *'bgaA* and *'spr0564* are the genes that allow for insertion into the *S. pneumoniae* genome by a double crossover event. **B:** Electrophoresis gel of a PCR screen for pJWV25 in *S. pneumoniae* transformant gDNA. The expected product of the PCR was 420bp indicated by the yellow arrow.

3.5.2 Production of Chemically Defined Media and Preliminary Growth Curves

In experiments designed to investigate cellular pathways, it is an invaluable tool to have a chemically defined media (CDM) that allows you to remove or add components in order to test various conditions. CDM should allow for bacterial growth curves that are comparable to the complex media that is commonly used to grow that organism. Another reason why CDM is so valuable as an experimental tool is due to the auto fluorescent nature of complex media. This attribute leads to complications when performing analysis on quantitative measurements that are meant to read the fluorescence of a conjugated toxin or genetically modified bacterium.

A chemically defined medium was made to the specifications found in the supplementary information in Appendix I. As the complete CDM is not stable for long

periods of time, the components are created in mass quantities then frozen to allow for replication. In the case of the following experiment a small batch of 100ml was used.

To test the CDM two well studied and characterized strains of *S. pneumoniae*, D39 and TIGR4, were chosen as there is a variety of literature and mutants are available for each strain. D39 is a virulent serotype 2 strain first used by Fredrick Griffith in 1928. TIGR4 is a virulent serotype 4 clinical isolate first isolated by Aaberge in 1995. Either of these strains would provide a good genetic background for future experiments.

Standard inocula in CDM were first made for both wild type *S. pneumoniae* strains, D39 and TIGR4, so there would be little to no carryover of nutrients from the complex medium into the growth curves. A growth curve was performed in a microplate reader with a duplicate culture growing in a 37^{o}C water bath which allowed for viable counting (described in 2.3.1). The results of the duplicate culture grown in 10ml of either CDM or BHI complex media are shown in Figure 3.19 B and C. The results show that there was growth of both strains in both conditions at a steady rate as determined by CFU/ml calculated by viable counting. The cultures in BHI grew to a greater OD_{600} than the CDM cultures.

The growth curve from the plate reader (Figure 3.19A) showed very different results to the cultures grown in larger volumes of media in the water bath. The cultures in BHI were found to have a typical growth curve with a small lag phase, an exponential or log phase and a stationary phase around OD_{600} 0.6 which is typical for *S. pneumoniae* as this is when autolysis begins. On the other hand, the absorbance profile for the strains grown in CDM did not resemble a typical growth curve. The D39 strain in CDM showed a short growth phase although this was much shorter the D39 grown in BHI. The cells grown in CDM died after only 4 hours of incubation. The TIGR4 strain did not appear to ever start growing properly in the CDM.

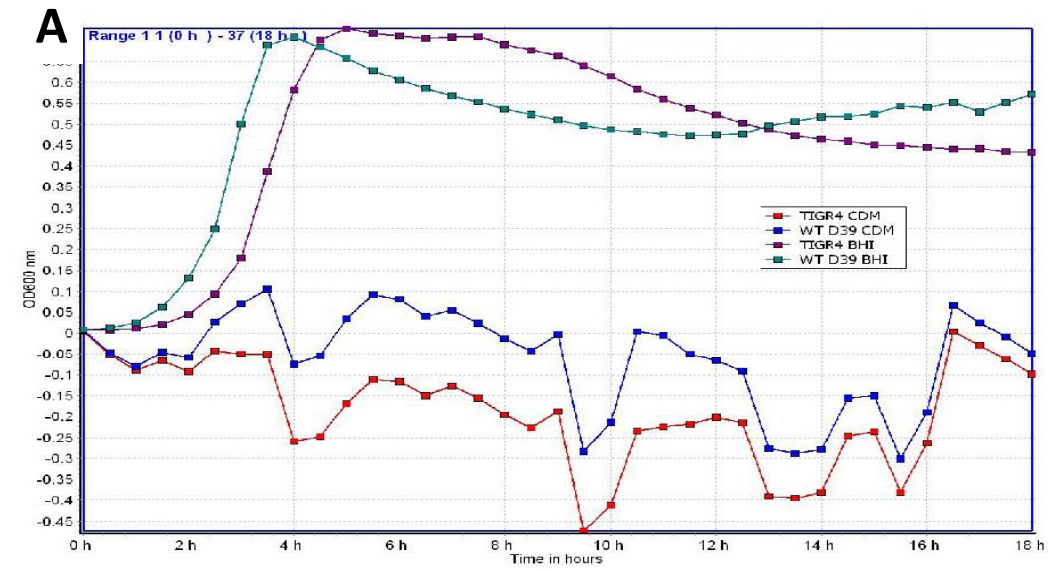

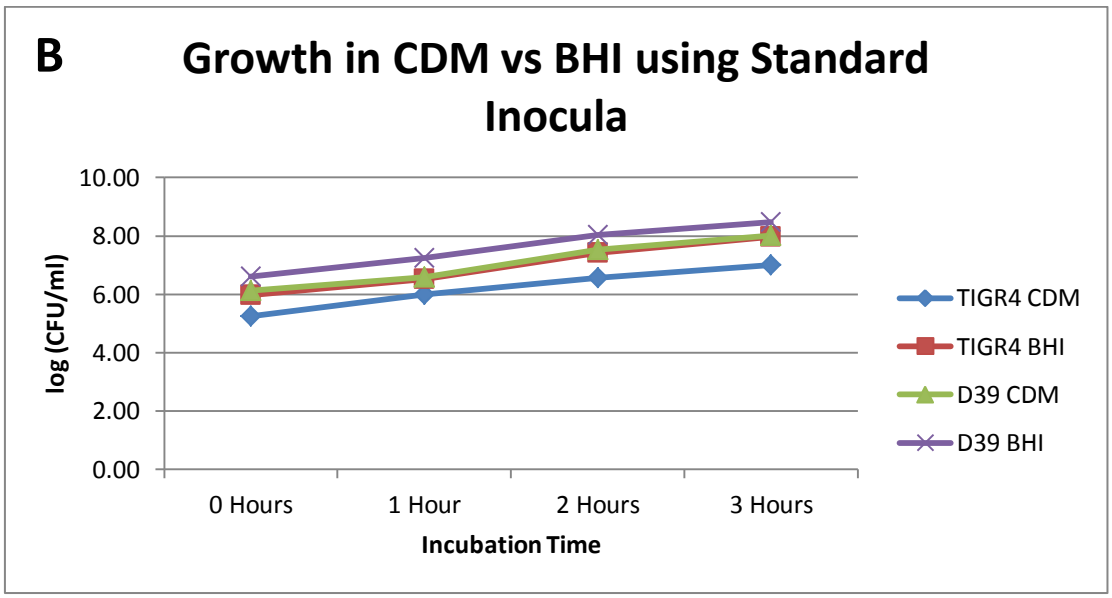

Figure 3.19 Growth Curve of CDM vs. BHI cultures A) Graph representing the growth of TIGR4 and D39 *S. pneumoniae* in either BHI or CDM over an 18 hour growth period in a 96 well plate at 37^{o}C and 5% CO_2 **B)** Graph of the CFU/ml of *S. pneumonaie* strains grown in parallel with the plate reader experiment. These were grown in a 37^{o}C water bath from the same OD_{600} 0.6 standard inoculum added to the 96 well plate.

Chapter 4: Discussion

4.1 Purification of proteins

A goal of pneumococcal research is the development of therapeutic agents such as new antibiotics and vaccines to aide in curing and preventing pneumococcal disease throughout the world. An important part of this process is to understand the interactions of the *Streptococcus pneumoniae* with the host cell. By illuminating the various effects the bacterium has on its host, one can target virulence factors or processes that lead to disease. In the case of *Streptococcus pneumoniae,* the pore forming toxin it produces, pneumolysin, has been shown to be important in the pathogenesis of disease caused by this organism. PLY has been found to be important for the growth of the bacteria *in vivo* as well as for the overall survivability of the host once infection has occurred (Benton, 1995; Berry, 1989). Not only is PLY an important virulence factor of the *S. pneumoniae,* it has also been identified for its potential use in vaccine development due to its existence in almost all clinical isolates of pneumococcus, this may allow for the development of a non-serotype specific pneumococcal vaccine (Kadioglu, 2008).

As *S. pneumoniae* produces many virulence factors which aid in its capacity to cause disease, the first step in elucidating PLY specific effects was to purify the toxin itself for use in various experiments that would allow for the testing of the effects of the toxin alone. Once a protein is purified, various quality checks must be also be performed to ensure that the purified protein is the expected size, there are no obvious contaminants and is functional before moving forward with experimentation. As shown in results sections 3.1, western blots and Coomassie gels were run during and after the purification process using a polyclonal primary antibody targeted to pneumolysin. The protein purified was found to be approximately 57kDa in size, which was the expected size taking into account the size of the protein pneumolysin at 53kDa and the added His-tag. Although the protein preparation seems

clear of obvious contaminations, silver staining was also performed (not shown) to have increased sensitivity. A small spectrum of faint bands of various sizes did appear in silver staining. It is advised that the use of AEC for purification should remove the negatively charged LPS but specialized LPS testing would have been preferable due to the focus of this project on PLY and the fair amount of protein purified. If the LPS test showed any contamination, purification direct from *S. pneumoniae* may have to be investigated. Direct purification from *S. pneumonaie* would be more costly for time and resources and would result in a loss of ability to compare the purified batch to that of other lab stocks, which are recombinant protein.

As LPS is a common contaminant in *E. coli* based protein purification, a negative control was required to use in all cell based experiments. This negative vehicle would be the protein preparation minus the pneumolysin protein itself. The method of using magnetic nickel beads yielded a small batch of negative vehicle which was tested against a polyclonal antibody for pneumolysin in a western blot (Figure 3.4) The technique of generating a negative vehicle in larger batches so no variation could come into experimentation would have to be considered if a more in depth project arises from the foundations of this one. Also still unknown is why the pneumolysin protein eluted from the magnetic nickel beads was non haemolytic although this lack of functionality may be due to an interaction between pneumolysin and the imidazole in the elution buffer. Another possible explanation for the lack of haemolytic ability could be due to aggregation of pneumolysin monomers. The aggregates may prevent the protein from binding or changing conformation, both of which are important for the haemolysis of eukaryotic cells. Aggregation may also be the cause of the marked higher molecular band seen in Figure 3.4 which occurred in the pneumolysin eluted from the nickel beads. Also of note is the smearing that occurred in the lane of the gel where the

protein eluted from the nickel beads ran (Figure 3.4). This effect may be due to denaturation of the protein from excess time at room temperature.

To determine the functionality of PLY a combination of haemolytic assays and cell based toxicity assays were performed. The result of the haemolytic assays for PLY is shown qualitatively in Figure 3.5 and quantitatively in Figure 3.6. The haemolytic activity of WTPLY NC-01 was calculated as is standard when purifying pneumolysin and was found to be 6.4×10^5 HU/mg. However, a study by Benton et al. in 1997 suggested that the value of haemolytic activity of PLY did not affect the pneumococcal strains virulence or growth in an *in vivo* model of disease (Benton, 1997). So although many studies identify this value as part of the purification process haemolytic activity is perhaps more useful when it comes to comparing different structural mutants to identify how changes within the PLY sequence could change its function as a pore forming toxin.

Due to its toxicity to cells, PLY itself would not be safe to use in vaccine development so for both research and clinical purposes many truncated or mutated versions of PLY have been created that prevent its full functionality as a pore forming toxin. Some of the toxoids that have been created are, pdT (Berry, 1995), plD1 [Pd_{H367}] (Berry, 1995), plD2 (Goulart, 2013), and PdB (Paton, 1991). One toxoid version of PLY, named Δ6PLY due to a deletion of the 146^{th} and 147^{th} amino acids of the pneumolysin sequence, was developed by Kirkham et al in 2006 and had characteristics that would make it an ideal candidate for vaccine development (Kirkham, 2006). Δ6PLY was found to not be cytotoxic even at concentrations of 1000 times that of WTPLY. It was also discovered that the toxoid did not form functional pores but retained the immunogenic effects of PLY. This means that antibodies can be raised against PLY resulting in host protection without the damage caused by the wild type toxin

making this toxoid an invaluable tool for vaccine candidates and research studies involving living cells and tissues (Kirkham, 2006).

A variant of the Δ6PLY toxoid was produced by another member of the Mitchell lab, Graeme Cowan as detailed in his PhD thesis (Cowan, 2006). This variant, named Δ6eGFPPLY is an eGFP conjugated version of the toxoid that provides a tool for cell studies involving microscopy as the toxoid will be able to be easily visualized in the green fluorescence channel at eGFP's optimum wavelengths for excitation and emission of 488/509. The fluorescence conjugation grants the ability to track the toxoid in a live system and to perform various localization studies.

The aim of this research project was to determine host-pathogen interactions in the context of the pore forming PLY. The ability to utilize the Δ6PLY toxoid and its eGFP conjugated version, Δ6eGFPPLY, provides a useful tool in determining which effects are caused as a result of the pore formation or cytotoxicity of the wild type toxin compared to effects caused due to immune response cascades which are triggered by both the wild type toxin and the toxoid.

The purification process for both proteins resulted in high yields of each protein, approximately 18.5mg for Δ6PLY and 35mg for Δ6eGFPPLY. These proteins were diluted to approximately 1.0mg/ml stocks and frozen until required to prevent degradation. The quality control tests shown in Figures 4.7 and 4.8 came back with a strong band of each protein at the projected molecular weights and a lack of haemolytic activity which is expected for these toxoids as previously characterized by previous lab members (Kirkham, 2006; Cowan, 2006). These results provide a solid foundation for the use of these proteins in experiments with the confidence that they are relatively pure and functioning as expected.

4.2 Determining sublytic concentration of WTPLY

Much of the existing research on PLY is based upon the effects of PLY when it is at lytic concentrations in the host. This project was aimed more at how the host responds when PLY is present but at sublytic concentrations. To identify what dose of toxin was sublytic, cell based assays were performed to test the cytotoxicity of the WTPLY prepared. The lactate dehydrogenase assay is a commonly used assay to determine the permeability of cell membranes in response to toxin (Aguilar, 2009; Förtsch, 2011). LDH assays were used to test the membrane permeability due to pore formation and the results compared with MTT assays which are cell live/dead assays. The first type of cells used in these assays was L929 fibroblast cells which were chosen to test the method used as the cells are easy to grow and work with and allowed for comparison of the results to previous studies to further validate the WTPLY preparation. The MTT and LDH assays both showed sublytic concentrations of PLY to be approximately 0.1μg/ml (Figure 3.9). At this concentration, there was minimal cell death and almost no cell lysis. The concentration found in the results also agrees with sublytic concentrations used in studies in the literature (Iliev, 2007).

Distinguishing between lytic and sublytic concentrations of pore forming toxins is critical when applying lytic toxins to cells in the study of the effect of the toxin on triggering host cell pathways without killing the cells. If the concentration added to any experiment is in the lytic range of the toxin then the host cells will initiate pathways that are involved in committed death of the cell, where if a sublytic concentration of the toxin is added to an experiment the host cell may initiate more inflammation and emergency recovery pathways in an attempt to survive the attack. A study by Babiychuk et al. (2009) looks into the difference in commitment of host cells to apoptosis and death in response to streptolysin O, a member of the cholesterol dependent cytolysin pore forming toxin family related to pneumolysin. This study investigates the ability of a cell to cope with varying concentrations of streptolysin O

and shows that at certain concentrations the toxin overwhelms the host cell. The cell is therefore unable to repair itself leading to prolonged periods of ion oscillations or even cell death (Babiychuk, 2009).

Another important factor to consider is the concentrations of toxin that would be found in infection and if these would be really as high as the concentrations used in most studies *in vitro*. If the concentrations vary significantly the results of the experiments performed will not reflect what is happening in the live system.

The LDH assays applied to A549 cells showed that the sublytic concentration when applied to lung epithelial cells for the batch of pneumolysin purified for this MSc was 0.1µg/ml [Figure 3.10]. This concentration agrees with the sublytic concentration described in many published articles as well as the L929 fibroblast experiments performed and will therefore be the concentration utilized in future experiments (Aguilar, 2009; Iliev, 2007; Förtsch, 2011; Shin, 2010).

4.3 Cytotoxic effects of PLY and Δ6PLY toxoid in A549 lung epithelial cells

Microscopy was performed to give a qualitative rather than quantitative evaluation of the effects of toxin exposure on A549 cells [Figures 3.11 and 3.12]. For the first experiment exposing A549 cells to eGFPPLY, the concentration of fluorescent toxin used was 1.1µM, 11.1µM and 111.5µM. The concentrations used should have been 1.8µM, 18.1µM and 180.6µM to match the molarity of WTPLY at sublytic and lytic concentrations. This experiment however failed to correct for the eGFP molecule which accounts for approximately a third of the size of the eGFPPLY molecule. This experiment nevertheless gives an at a glance example of how a relatively low concentration of pneumolysin causes substantial damage to host cells leading to cell death.

The Δ6eGFPPLY toxoid, which was adjusted to the proper concentrations based on molarity, showed very different results. This toxoid lacks the ability to form functional pores and as a result the host cells can tolerate at least 100 times the dose of Δ6eGFPPLY without showing signs of cell death such as membrane blebbing and cell rounding which can be seen in the fully functional eGFPPLY toxin [Figure 3.12]. As mentioned above, this toxoid will prove valuable in distinguishing pathways initiated by cytotoxicity and those caused by immune reactions as the toxoid has been proven to be as immunogenic as its wild type predecessor (Kirkham, 2006).

4.4 Effects of PLY on E-cadherin and F-actin in A549 lung epithelial cells

Various studies have demonstrated pathways involved in cell to cell contacts are affected by the CDC toxin pneumolysin. A study involving E-cadherin was performed by Beisswenger et al (2007) and demonstrated colocalization between *S. pneumoniae* and E-cadherin in human bronchial epithelial cells (Beisswenger, 2007). The observed colocalization may indicate a step in the invasion process of *S. pneumoniae*.

Another study by Inoshima et al. (2011) showed degradation of E-cadherin protein when A549 cell monolayers were exposed to pneumolysin at concentrations of 0.1μg/ml to 20μg/ml as demonstrated by an increase in cleavage of the C-terminal fragment of E-cadherin respective to increasing concentrations of WTPLY (Inoshima, 2011). Figure 3.16 shows the result of an experiment in which A549 cell monolayers were exposed to a sublytic, 0.1μg/ml concentration and a lytic, 10μg/ml concentration of pneumolysin. E-cadherin was subsequently probed for and in agreement with the methods in the Inoshima paper (2011). The lytic concentration of PLY showed cleavage of E-cadherin as demonstrated by lack of an E-cadherin band at 100kDa, whereas the sublytic concentration of PLY had E-cadherin bands were present at about the same intensity as A549 lysate controls [Figure 3.16B Lanes 1 and 4 for A549 cells exposed to sublytic pneumolysin and lanes 6 and 7 for whole cell lysate

controls]. The next step would be to probe for E-cadherin using PLY time and dose curves paying even greater attention to equal loading in order to identify what time exposure or concentration is required to cleave E-cadherin. Also the non-specific cross reactivity by the 800nm secondary antibody will have to be addressed for clarity of the results and to ensure that densitometry is as accurate as possible when determining band intensity.

Immunofluorescence was also performed to try to qualitatively detect the degradation of E-cadherin when A549 cells were exposed to pneumolysin. The Inoshima group (2011) did not attempt any such qualitative experiments when testing the pore forming toxin, α-hemolysin from *S. aureus*.

Figure 3.13 shows the results of the E-cadherin immunofluorescence. There is no control that can be shown for comparison as this was a preliminary experiment just to see if E-cadherin staining could be accomplished. Figure 3.13 shows E-cadherin can be detected in A549 cell monolayers but the signal intensity was poor and staining was not specific to cell junctions as was expected and therefore the results were not suitable for further analysis. Both the E-cadherin immunofluorescence and the western blotting protocols will have to continue to be optimized before results that could help understand the interaction between PLY and E-cadherin can be elucidated. From the results acquired so far, it is thought that the immunofluorescence work may require the use of a chemically conjugated version of the toxin as used in the Hupp et al. (2012) paper to increase the fluorescence intensity that is lacking in the eGFP version of the toxin as even utilizing concentrations 3x higher than the sublytic level did not increase toxin intensity to an adequate level. The chemical conjugation may also allow for further magnification of the cells without the extensive photo bleaching seen in the performed experiments. To aid in seeing the E-cadherin protein, the immunoprecipitation step performed by Inoshima et al. (2011) may have to be performed to concentrate the protein to a level in which the bands can be more easily distinguished

especially when being visualized against a high staining background on the blot. For the immunofluorescence, the staining protocol and or the monolayer growth may have to be adjusted to result in brighter staining of the E-cadherin. A different E-cadherin antibody may also need to be investigated as even at a high concentration only a low E-cadherin signal could be seen.

The immunofluorescence targeting F-actin proved successful [Figures 3.14 and 3.15]. Although preliminary in nature and these experiments were designed to test the use of the reagents and protocols from the papers by the Iliev group (Förtsch, 2011; Hupp, 2012) before any multiplex staining would be attempted. The discovery of the difference in staining intensity between the wild type toxin conjugated to eGFP and the Δ6eGFPPLY toxoid was interesting as this seems to be the opposite effect as recorded in the Förtsch et al. (2011) paper. The results of the Förtsch et al study showed that PLY interacting with actin provided more intensely stained F-actin fibres than cells not treated by the toxin. Therefore, one would predict the wild type conjugated PLY would result in more intense F-actin staining than the Δ6eGFPPLY toxoid which is unable enter the cell and colocalize with actin thereby initiating and downstream pathways that would result in more intense fibre staining. The group also showed that the Δ6PLY toxoid did not cause displacement and retraction of cells that was seen in PLY treated cells which indicate the cells treated with PLY underwent extensive cytoskeletal changes to allow for the increase in focal adhesion size, migration and morphological changes in the astrocyte cells (Förtsch, 2011). The F-actin fibres do look more organized in the eGFPPLY treated cells [Figures 3.17 and 3.18].

The goal of the immunofluorescence experiments was to incorporate a triplex staining protocol so that the eGFP conjugated PLY toxin location can be seen alongside E-cadherin and F-actin proteins to determine PLY effects on both of these proteins simultaneously. The

results above show that the F-actin component is working well and with a different E-cadherin antibody and chemical conjugation of the toxin the triplex staining will be achieved. Hopefully, with higher resolution, any colocalization will be evident such as previously shown between PLY and F-actin in the study performed by Hupp et al. (2012). This line of investigation is to discern whether or not PLY interacts with these proteins directly or if PLY indirectly activates signalling cascades that affect the pathways these proteins are involved in thereby leading to bacterial invasion through tissue.

4.5 Effect of pneumolysin and capsule on adherence of *S. pneumoniae* to A549 lung epithelial cells

The purpose of the adherence assay experiments was to determine the best bacterial model for further adherence and invasion assays. Various studies have shown that encapsulated *S. pneumoniae* have a decreased adherence and invasion compared to unencapsulated versions (Marriott, 2011; Beisswenger, 2007 respectively). Beisswenger et al. (2007) also showed that a pneumolysin negative version of *S. pneumoniae* did not significantly increase the time of transepithelial migration compared to wild type *S. pneumoniae*, indicating the PLY may not make a large contribution to tissue invasion. The adherence experiments performed were to test capsule and PLY under the same conditions and to confirm the results of the various studies while testing in the cell line of interest, A549 lung epithelial cells to determine the best strain to use in experimentation going forward. As shown in Figure 3.17, D39 encapsulated, serotype 2, clinical isolate was directly compared with a PLY negative derivative of D39, D39 PLY STOP, in which a premature stop codon was created by mutation resulting in a non-functional PLY protein, FP22, a D39 mutant strain created and characterized by Pearce et al (2002) by insertion of a kanamycin resistance cassette into the capsule locus of D39 generating a nonencapsulated version of the parent type and R6 which is an unencapsulated, avirulent laboratory strain related to the D39 strain. This allowed for the testing of nonencapsulated vs. encapsulated and PLY vs. no PLY all in one.

The results shown in Figure 3.17 agree with the previously reported results found in the literature. One such result is that non-encapsulated FP22 adhered to cells slightly better than the encapsulated parent strain D39. The approximate percentage of adherence and relationship of the two strains agrees with the study performed by Marriott et al. (2011), although unlike the Marriott study no statistical significance was found as the p-value only reached 0.145 due to a higher percent adherence seen in the D39 encapsulated strain in this set of experiments. Another pertinent result was that the lack of PLY did not significantly affect the adherence of *S. pneumoniae* to A549 cells, which agrees with the result found when PLY and PLY negative strains were tested in human bronchial cells in the Beisswenger et al. (2007) paper. Probably the most important thing to remember is that there is a wide variance between the percent adherence found between the encapsulated and unencapsulated strains as well as between D39 and its mutants and the R6 nonvirulent D39 derivative. The difference in adherence between FP22 and R6, both of which are nonencapsulated is interesting and may be worth investigating further as to whether R6 has other factors such as an increased expression of adherins that give it the greater ability to adhere to A549 cells..

These discoveries will allow accurate planning of further experiments for not only what strain to use but also what parent strain should be utilized if mutants are to be generated in the interest of studying a specific pathway. For example, FP22 might want to be used as a background rather than D39 itself if investigating pathways of adherence and invasion as this may highlight any differences between the mutant and parent strain. As seen with D39 and D39 PLY STOP, the encapsulated strains ability to adhere is so close that any difference may be lost due to a general lack of adherence caused by the polysaccharide capsule whereas the difference in adherence may be found to be a statistically significant result if a more adherent strain was used. The effects of removing the capsule must also be considered carefully to determine if it is a reasonable trade off as lack of a capsule changes many aspects of bacterial

behaviour and the host's behaviour to the organism. Van der Windt et al. (2012) showed that a unencapsulated D39 had a greater resistance to killing by neutrophil proteases than the encapsulated D39 which combined with their increased ability to adhere may be why more unencapsulated *S. pneumoniae* are found on mucosal surfaces than encapsulated strains.

4.6 Host-Pathogen Interactions and Generation of a Fluorescently Tagged Pneumolysin

The applications of green fluorescence protein (GFP) have been widely used in protein localisation, cell labelling, DNA and RNA labelling and promoter tracking (Chudakov, 2010). Until recently, the use of fluorescence in the study of *S. pneumoniae* has been limited. This may be due to the fact that it is notoriously hard to visualize GFP in *S. pneumoniae* due to their preference for low oxygen and their creation of acidic environments, both of which negatively affect the performance of GFP (Acebo, 2000). A few recent studies in the pneumococcal field have begun to develop molecular toolboxes that include fluorescence in the study of pneumococci (Eberhardt, 2009; Henriques, 2013; Holmes, 2012). One such study, Eberhardt et al. 2009, has been investigated for possible use in the current study. Of the two plasmids described in this study, the plasmid pJWV25 is most relevant as it allows construction of an N-terminal fusion between a chosen protein to a high intensity variant of GFP, called GFP+. The link to the N-terminal end of PLY is crucial for use in this project as any large proteins such as GFP+ cannot be linked to the C-terminal domain of PLY as the C-terminal domain is the essential in the toxin binding to target cells and therefore a large protein would likely interfere with any toxin-host interaction and downstream signalling cascades which are the main focus of this project (Marriott, 2008). Also the utilization of a double crossover event to integrate the fusion gene into the pneumococcal chromosome is advantageous as it allows for the generation of a more stable mutant which expresses the fusion protein (Eberhardt, 2009). The plasmid pJWV25 contains a zinc inducible promoter that was originally introduced into the plasmid pMP2-2 (Kloostermann, 2007) which is the

precursor of pJWV25. Although an inducible promoter is potentially useful, the concentration of zinc (0.15mM) required to initiate the production of the GFP+ is high enough to be lethal mammalian cells and is therefore not suitable for studies of host-pathogen interactions. For use in this project, a new promoter would have to be inserted into the pJWV25 plasmid to replace the zinc inducible promoter. The promoter chosen for this will be a constitutive promoter, P2, isolated and characterized by a member of the Pneumococcal Research Group (Herbert, 2012). Although this promoter is not inducible, it will allow constitutive expression of fusion constructs for studies involving the localisation of PLY in cell and animal systems.

The introduction of pJWV25 into *S. pneumoniae* was attempted for a number of reasons. This plasmid was designed in the Veening lab and needed to be tested in the pneumococcal strains of interest, D39 and TIGR4. The *S. pneumoniae* pJWV25 clone would give a GFP+ mutant that would fluoresce when induced with zinc. Although the zinc concentration required to induce protein production is too high to be used with mammalian cells, this experiment was performed to ensure the protein induction system designed in the plasmid worked with the strains of interest before switching out the promoter for P2 which could be utilized in a live cell system. The constructs could also be used in pneumolysin localisation studies with respect to bacterial cells alone as the method of release of PLY from the bacterial cell is still in unclear. The results show a screening PCR using primers designed in Eberhardt et al. 2009 that will amplify a section of pJWV25 if it is present within the DNA of interest (Eberhardt, 2009). Figure 3.17 shows that a product was amplified from the chromosome of D39 *S. pneumoniae*. This is a good indication that the transformation of the plasmid into *S. pneumoniae* was successful. However, to confirm this observation sequencing and possibly fluorescence microscopy should be done to further verify these results.

Other possible fluorescence constructs were also considered as described by Henriques et al. 2013. This study illustrates various florescent constructs that could be used as

an alternative to GFP to counteract the difficulties with using GFP in *S. pneumoniae* studies as described above due to the organism favouring low oxygen environments. The other possible fluorescent fusions that could be used were mCherry, Citrine and CFP which would be expressed via a plasmid (Henriques, 2013). The reason the Eberhardt (2009) GFP+ construct was ultimately pursued was due to the strength of the plasmid construction with the favourable flexible linker region and double crossover event to incorporate the fluorescent tag into the genome which would result in a more stable mutant as *S. pneumoniae* frequently favours genetic recombination and often ejects plasmids.

The growth curves with CDM were to test that the defined media allowed the growth of TIGR4 and D39. These two strains were chosen as they are well characterized in various assays throughout literature. The results [Figure 3.19] show the successful growth of these strains in CDM, although at a lesser degree than BHI, in a water bath culture. However, the growth of these strains was not successful in the 96 well plate during a growth curve experiment. A possible reason for the lack of growth could be due to the volume in which these strains were allowed to grow for the 18 hour period. There may be some difference in the nutrient proportions when scaled down to 200µl for use in a 96 well plate that are corrected in larger volumes such as the 10ml universals. There may also be something said for the evaporation effects that occur in plates that do not in closed universals. This line of thought is however pure speculation and if in the future CDM is to be used in 96 well format for multiplex testing it will have to be further investigated. For the purpose of this project, CDM was mainly to be used for microscopy work and will be used for microscope slides or in 35mm dishes to prevent the auto-fluorescence that occurs in BHI. Hopefully at the volumes required for these experiments the lack of growth will not be seen and the benefits will therefore outweigh the negatives of utilizing this media.

4.7 Summary

This project aimed to study some of the interactions between the pore forming toxin pneumolysin and human host cells. This study was focused on the studying the interactions with regards to the epithelial cell barrier to further understand how *S. pneumoniae* invades the host changing it from a commensal organism to an invasive one. The experiments in this study were designed to first create an optimized testing environment then to test the interaction of PLY with host cell epithelial barriers and the pathways that regulate them.

Chemically defined media was prepared and successfully tested for later use in fluorescent microscopy studies to reduce background fluorescence that occurs with standard media. Optimization of a plasmid for expression of a fluorescently conjugated pneumolysin produced in *S. pneumoniae* rather than a Gram negative equivalent was begun for later use in localisation studies to see if PLY co-localises or directly interacts with any epithelial proteins. Adherence experiments showed that the optimal background strain for investigation into invasion would be one that is encapsulated as the adherence to the host is much greater than strains that have a polysaccharide capsule. The preliminary fluorescence experiments led to the successful staining of F-actin fibres and also determined the highest concentration of PLY that could be used before lytic effects would occur in the host cell.

There were difficulties in this project such as finding a suitable E-cadherin antibody that would be able to fluoresce without significant photo bleaching as high magnification was to be used. Also cloning the pJWV25 plasmid into the desired strains of *S. pneumoniae* successfully proved difficult as spontaneous antibiotic resistant mutants were often the result rather than the actual incorporation of the plasmid. However, despite the issues a foundation for further successes seems to have been laid and with further time and resources more definitive and progressive results would have hopefully been on the horizon.

4.8 Future Work

The experiments completed during the course of this master's project open up a variety of future work that can build upon the foundation of the results shown discussed in this thesis.

The purification of the proteins and the establishment of sublytic concentrations allow for future cell based assays. A more in depth investigation of apoptotic and repair pathways triggered by sublytic vs lytic amounts of pneumolysin can be designed and carried out. Also one can build upon the F-actin and E-cadherin work shown in this paper and continue with time and dose curves to see what concentration of pneumolysin causes the degradation of E-cadherin and if pneumolysin effects F-actin in a similar way. Co-localization studies can also be pursued with further adjustments to the E-cadherin immunofluorescence as the F-actin staining proved successful and as there is a large successful batch of Δ6eGFPPLY already available only a batch of eGFPPLY would be required to apply fluorescent toxin to the cell monolayers. The CDM media can be applied to perhaps employ any live cell imaging to avoid auto fluorescence.

The adherence assays showed that a noncapsular version of D39 could be used to investigate transepithelial migration thru invasion assays. Although the adherence assays indicated PLY does not play a major role in adherence it may be that it plays a greater role in invasion of epithelial barriers.

The pJWV25 plasmid work could also be pursued further to allow for a constitutive promoter of fluorescently tagged PLY in its natural host which would be useful for any experiments utilizing live bacteria which would create a more realistic experimental model than using protein purified in a Gram negative bacterium.

Appendix I Recipes

CDM Buffer	
Chemical	**Amount**
Na-B-glycerophosphate	21 g
KH_2PO_4	1 g
$(NH_4)_3$ citrate	0.6 g
Na-acetate	1 g
Dissolved in 800 mL dH_2O, pH 6.4 with 1 M HCL	

Metal Mixture	
Chemical	**Amount**
$MgCl_2 \cdot 6H2O$	4 g
$CaCl_2$	0.74 g
$ZnSO_4 \cdot 7H2O$	100 mg
$CoCl_2 \cdot 6H2O$	50 mg
$CuSO_4 \cdot 5H20$	2 mg
Dissolved in 200 mL dH_2O, pH 7.0	

Vitamin Mixture	
Chemical	**Amount**
Pyridoxal-Cl	40 mg
Thiamine Cl2	20 mg
Riboflavin	20 mg
Ca-pantothenate	20 mg
Biotin	2 mg
Folic acid (stored in dark)	20 mg
Niacin amide	20 mg
Dissolved in 200 mL dH_2O, pH 7.0	

Complete DMEM

176 ml Dulbecco's Modified Eagle Medium (Sigma)

20 ml Fetal Bovine Serum (Gibco)

2 ml Penicillin/Streptomycin (Sigma)

2 ml L-glutamine (Sigma)

Lysis buffer (E-cadherin experiments) modified from Inoshima et al 2011

10mm Tris pH 7.4 (Fisher Scientific)

150mM NaCl (VWR)

2mM EDTA (Fisher Scientific)

0.5% IGEPAL CA-630 (Sigma)

1% Triton X-100 (Sigma)

cOmplete EDTA free protease inhibitor cocktail tablet (Roche)

up to 50 ml in dH_2O

TBST

20mM Tris (Fisher Scientific)

137mM NaCl (VWR)

0.1% Tween (Sigma)

pH 7.6

High salt TBST

145ml of 5M NaCl (VWR)

Up to 2L of TBST

TBS

20mM Tris (Fisher Scientific)

137mM NaCl (VWR)

pH 7.6

4x Reducing SDS PAGE sample buffer

3.75ml 1M Tris-HCl pH 6.8

6ml glycerol (Fisher Scientific)

1.2g SDS (Fisher Scientific)

0.93g DTT (Sigma)

6mg bromophenol blue (BDH Biosciences)

Up to 15ml with dH_2

Appendix II Strains Used in this Study

D39 = serotype 2 *S. pneumoniae* strain used in the 1928 experiment by Frederick Griffith and Avery et al 1944.

D39 PLY STOP = D39 mutant in which the PLY gene has a premature stop codon resulting in a non functional toxin created by Graeme Cowan (2006) for use in his PhD thesis. This was accomplished using the Janus technique described in Sung et al. 2001.

D39 FP22 = acapsular D39 created by Pearce et al. 2002 by insertion of a Kanamycin cassette deleting the capsule locus

R6 = laboratory, acapsular, avirulent descendent of D39 serotype 2 strain used in the study by Avery et al 1944

TIGR4 = Serotype 4 clinical isolate of *S. pneumoniae.* Strain was isolated in the study by Aaberge et al. 1995.

References

Aaberge, I.S., Eng, J., Lermark, G. and Løvik, M. (1995). Virulence of *Streptococcus pneumoniae* in mice: a standardized method for preparation and frozen storage of the experimental bacterial inoculum. *Microbial Pathogenesis 18*(2), 141-152. doi:10.1016/S0882-4010(95)90125-6

Acebo, P., Nieto, C., Corrales, M. a, Espinosa, M., & López, P. (2000). Quantitative detection of Streptococcus pneumoniae cells harbouring single or multiple copies of the gene encoding the green fluorescent protein. *Microbiology (Reading, England)*, *146 (Pt 6)*, 1267–73. Retrieved from http://www.ncbi.nlm.nih.gov/pubmed/10846206

Aguilar, J. L., Kulkarni, R., Randis, T. M., Soman, S., Kikuchi, A., Yin, Y., & Ratner, A. J. (2009). Phosphatase-dependent regulation of epithelial mitogen-activated protein kinase responses to toxin-induced membrane pores. *PloS One*, *4*(11), e8076. doi:10.1371/journal.pone.0008076

Arulanandam, R., Vultur, A., Cao, J., Carefoot, E., Elliott, B. E., Truesdell, P. F., … Raptis, L. (2009). Cadherin-cadherin engagement promotes cell survival via Rac1/Cdc42 and signal transducer and activator of transcription-3. *Molecular Cancer Research : MCR*, *7*(8), 1310–27. doi:10.1158/1541-7786.MCR-08-0469

Avery, O.T., Macleod, C.M, and McCarty, M. (1944). Studies on the Chemical Nature of the Substance Inducing Transformation of Pneumococcal Types. *Journal of Experimental Medicine 79*(2), 137-158.

Babiychuk, E. B., Monastyrskaya, K., Potez, S., & Draeger, a. (2009). Intracellular Ca (2+) operates a switch between repair and lysis of streptolysin O-perforated cells. *Cell Death and Differentiation*, *16*(8), 1126–34. doi:10.1038/cdd.2009.30

Balachandran, P., Hollingshead, S. K., Paton, J. C., & Briles, D. E. (2001). The Autolytic Enzyme LytA of *Streptococcus pneumoniae* Is Not Responsible for Releasing Pneumolysin, *183*(10), 3108–3116. doi:10.1128/JB.183.10.3108

Beisswenger, C., Coyne, C. B., Shchepetov, M., & Weiser, J. N. (2007). Role of p38 MAP kinase and transforming growth factor-beta signaling in transepithelial migration of invasive bacterial pathogens. *The Journal of Biological Chemistry*, *282*(39), 28700–8. doi:10.1074/jbc.M703576200

Benton, K. a, Everson, M. P., & Briles, D. E. (1995). A pneumolysin-negative mutant of *Streptococcus pneumoniae* causes chronic bacteremia rather than acute sepsis in mice. *Infection and Immunity*, *63*(2), 448–455. Retrieved from http://www.pubmedcentral.nih.gov/articlerender.fcgi?artid=173016&tool=pmcentrez&rendertype=abstract

Benton, K. A., Paton, J. C., & Briles, D.E. (1997). Differences in Virulence for Mice among *Streptococcus pneumoniae* Are Not Attributable to Differences in Pneumolysin Production, *65*(4), 1237–1244.

Berry, a M., Yother, J., Briles, D. E., Hansman, D., & Paton, J. C. (1989). Reduced virulence of a defined pneumolysin-negative mutant of *Streptococcus pneumoniae*. *Infection and Immunity*, *57*(7), 2037–2042. Retrieved from http://www.pubmedcentral.nih.gov/articlerender.fcgi?artid=313838&tool=pmcentrez&rendertype=abstract

Berry, a M., Alexander, J. E., Mitchell, T. J., Andrew, P. W., Hansman, D., & Paton, J. C. (1995). Effect of defined point mutations in the pneumolysin gene on the virulence of

Streptococcus pneumoniae. *Infection and Immunity*, *63*(5), 1969–74. Retrieved from http://www.pubmedcentral.nih.gov/articlerender.fcgi?artid=173251&tool=pmcentrez&rendertype=abstract

Braun, L., Nato, F., Payrastre, B., Mazié, J. C., & Cossart, P. (1999). The 213-amino-acid leucine-rich repeat region of the listeria monocytogenes InlB protein is sufficient for entry into mammalian cells, stimulation of PI 3-kinase and membrane ruffling. *Molecular Microbiology*, *34*(1), 10–23. Retrieved from http://www.ncbi.nlm.nih.gov/pubmed/10540282

Cassidy, S. K. B., & O'Riordan, M. X. D. (2013). More than a pore: the cellular response to cholesterol-dependent cytolysins. *Toxins*, *5*(4), 618–36. doi:10.3390/toxins5040618

Clarke, T.B., Francella, N., Huegel, A., and Weiser, J.N. (2011). Invasive Bacterial Pathogens Exploit TLR-Mediated Downregulation of Tight Junction Components to Facilitate Translocation across the Epithelium. *Cell Host and Microbe 9*, 404-414. doi:10.1016/j.chom.2011.04.012

Chudakov, D. M., Matz, M. V, Lukyanov, S., & Lukyanov, K. A. (2010). Fluorescent Proteins and Their Applications in Imaging Living Cells and Tissues, 1103–1163. doi:10.1152/physrev.00038.2009.

Cockeran, R., Theron, A.J., Steel, H.C., Matlola, N.M., Mitchell, T.J., Feldman, C. and Anderson, R. (2001). Proinflammatory Interactions of Pneumolysin with Human Neutrophils. *The Journal of Infectious Diseases 183*(4), 604-11. doi:10.1086/318536

Cowan, Graeme. (2006) Studies of the Cholesterol-dependent Cytolysins . Thesis.

University of Glasgow, 2006. Glasgow: University of Glasgow.

Desai, R. a, Gao, L., Raghavan, S., Liu, W. F., & Chen, C. S. (2009). Cell polarity triggered by cell-cell adhesion via E-cadherin. *Journal of Cell Science*, *122*(Pt 7), 905–11. doi:10.1242/jcs.028183

Eberhardt, A., Wu, L. J., Errington, J., Vollmer, W., & Veening, J.-W. (2009). Cellular localization of choline-utilization proteins in *Streptococcus pneumoniae* using novel fluorescent reporter systems. *Molecular Microbiology*, *74*(2), 395–408. doi:10.1111/j.1365-2958.2009.06872.x

Förtsch, C., Hupp, S., Ma, J., Mitchell, T. J., Maier, E., Benz, R., & Iliev, A. I. (2011). Changes in astrocyte shape induced by sublytic concentrations of the cholesterol-dependent cytolysin pneumolysin still require pore-forming capacity. *Most*, *3*(1), 43–62. doi:10.3390/toxins3010043

Gonzalez, M.R., Bischofberger, M., Pernot, L., van der Goot, F.G., & Frêche, B. (2007). Bacterial pore-forming toxins: The (w)hole story?. *Cellular and Molecular Life Sciences*, 65, 493-507. doi:10.1007/s00018-007-7434-y

Goulart, C., da Silva, T. R., Rodriguez, D., Politano, W. R., Leite, L. C. C., & Darrieux, M. (2013). Characterization of protective immune responses induced by pneumococcal surface protein A in fusion with pneumolysin derivatives. *PloS One*, *8*(3), e59605. doi:10.1371/journal.pone.0059605

Guiral, S., Mitchell, T. J., Martin, B., & Claverys, J.-P. (2005). Competence-programmed

predation of noncompetent cells in the human pathogen *Streptococcus pneumoniae*: genetic requirements. *Proceedings of the National Academy of Sciences of the United States of America*, *102*(24), 8710–5. doi:10.1073/pnas.0500879102

Henriques, M. X., Catalão, M. J., Figueiredo, J., Gomes, J. P., & Filipe, S. R. (2013). Construction of improved tools for protein localization studies in *Streptococcus pneumoniae*. *PloS one*, *8*(1), e55049. doi:10.1371/journal.pone.0055049

Herbert, Jenny. *Genetic regulation of virulence in Streptococcus pneumoniae*. Thesis. University of Glasgow, 2012. Glasgow: University of Glasgow, 25 April 2013.

Hiller, N.L., Janto, B., Hogg, J.S., Boissy, R., Yu, S., Powell, E., Keefe, R., Ehrlich, N.E., Shen, K., Hayes, J., Barbadora, K., Klimke, W., Dernovoy, D., Tatusova, T., Parkhill, J., Bentley, S.D., Post, J.C., Ehrlich, G.D., Hu, F.Z. (2007). Comparative Genetic Analyses of Seventeen *Streptococcus pneumoniae* Strains: Insights into the Pneumococcal Supragenome. *Journal of Bacteriology 189*(22), 8186-8195. doi:10.1128/JB.00690-07

Holmes, Ashleigh. *Characterising Virulence Factors from Pathogenic Bacteria Using Fluorescent Reporters*. Thesis. University of Glasgow, 2012. Glasgow: University of Glasgow, 2012. *Glasgow Theses Service*. University of Glasgow, 17 Apr. 2012. Web. 05 June 2013. <http://theses.gla.ac.uk/3317/>.

Hupp, S., Förtsch, C., Wippel, C., Ma, J., Mitchell, T. J., & Iliev, A. I. (2012). Direct Transmembrane Interaction between Actin and the Pore-Competent, Cholesterol-Dependent Cytolysin Pneumolysin. *Journal of molecular biology*, *425*(3), 636–646. doi:10.1016/j.jmb.2012.11.034

Iliev, A. I., Djannatian, J. R., Nau, R., Mitchell, T. J., & Wouters, F. S. (2007). Cholesterol-dependent actin remodeling via RhoA and Rac1 activation by the *Streptococcus pneumoniae* toxin pneumolysin. *Proceedings of the National Academy of Sciences of the United States of America*, *104*(8), 2897–2902. doi:10.1073/pnas.0608213104

Inoshima, I., Inoshima, N., Wilke, G. a, Powers, M. E., Frank, K. M., Wang, Y., & Bubeck Wardenburg, J. (2011). A Staphylococcus aureus pore-forming toxin subverts the activity of ADAM10 to cause lethal infection in mice. *Nature Medicine*, *17*(10), 1310–1314. doi:10.1038/nm.2451

Johnsborg, O. and Haverstein, L.S. (2009). Regulation of natural genetic transformation and acquisition of transforming DNA in *Steptococcus pneumoniae. FEMS Microbiology Review 33*, 627-642. doi:10.1111/j.1574-6976.2009.00167.x

Kadioglu, A., Coward, W., Colston, M. J., Hewitt, C. R. A., & Andrew, P. W. (2004). CD4-T-Lymphocyte Interactions with Pneumolysin and Pneumococci suggest a Crucial Protective Role in the Host Response to Pneumococcal Infection, *72*(5), 2689–2697. doi:10.1128/IAI.72.5.2689

Kadioglu, A., Weiser, J. N., Paton, J. C., & Andrew, P. W. (2008). The role of *Streptococcus pneumoniae* virulence factors in host respiratory colonization and disease. *Nature Reviews. Microbiology*, *6*(4), 288–301. doi:10.1038/nrmicro1871

Kirkham, L. S., Kerr, A. R., Douce, G. R., Paterson, G. K., Dilts, D. A., Liu, D., & Mitchell, T. J. (2006). Construction and Immunological Characterization of a Novel Nontoxic Protective Pneumolysin Mutant for Use in Future Pneumococcal Vaccines, *74*(1), 586–593. doi:10.1128/IAI.74.1.586

Kloosterman, T. G., Van der Kooi-Pol, M. M., Bijlsma, J. J. E., & Kuipers, O. P. (2007). The novel transcriptional regulator SczA mediates protection against Zn2+ stress by activation of the Zn2+-resistance gene czcD in *Streptococcus pneumoniae*. *Molecular microbiology*, *65*(4), 1049–1063. doi:10.1111/j.1365-2958.2007.05849.x

Koppe, U., Suttorp, N., & Opitz, B. (2012). Recognition of *Streptococcus pneumoniae* by the innate immune system. *Cellular Microbiology*, *14*(4), 460–466. doi:10.1111/j.1462-5822.2011.01746.x

Lawrence, S.L., Feil, S.C., Morton, C.J., Farrand, A.L., Mulhern, T.D., Gorman, M.A., Wade, K.R., Tweton, R.K., and Parker, M.W. (2015). Crystal structure of *Streptococcus pneumoniae* pneumolysin provides key insights into early steps of pore formation. *Scientific Reports 5*(14352). doi: 10.1038/srep14352

Lucas, R., Yang, G., Gorshkov, B. a, Zemskov, E. a, Sridhar, S., Umapathy, N. S., … Chakraborty, T. (2012). Protein kinase C-α and arginase I mediate pneumolysin-induced pulmonary endothelial hyperpermeability. *American journal of respiratory cell and molecular biology*, *47*(4), 445–453. doi:10.1165/rcmb.2011-0332OC

Malley, R., Henneke, P., Morse, S. C., Cieslewicz, M. J., Lipsitch, M., Thompson, C. M., Kurt-Jones, E., et al. (2003). Recognition of pneumolysin by Toll-like receptor 4 confers resistance to pneumococcal infection. *Proceedings of the National Academy of Sciences of the United States of America*, *100*(4), 1966–1971. doi:10.1073/pnas.0435928100

Marriott, H. M., Mitchell, T. J., & Dockrell, D. H. (2008). Pneumolysin: A double-edged

sword during the host-pathogen interaction. *Current Molecular Medicine*, *8*(6), 497–509. Retrieved from http://www.ingentaconnect.com/content/ben/cmm/2008/00000008/00000006/art00006?token=004a15417f9dc7e2a46762c6b672176666a70504956452a673f7b2f267738703375686f49b

Marriott, H. M., Gascoyne, K. a, Gowda, R., Geary, I., Nicklin, M. J. H., Iannelli, F., … Dockrell, D. H. (2011). Interleukin-1β regulates CXCL8 release and influences disease outcome in response to *Streptococcus pneumoniae*, defining intercellular cooperation between pulmonary epithelial cells and macrophages. *Infection and Immunity*, *80*(3), 1140–1149. doi:10.1128/IAI.05697-11

Marshall, J.E., Faraj, B.H.A, Gingras, A.R., Lonnen, R., Sheikh, M.A., El-Mezgueldi, M., Moody, P.C.E., Andrew, P.W. and Wallis, R. (2015). The Crystal Structure of Pneumolysin at 2.0 Å Resolution Reveals the Molecular Packing of the Pre-pore Complex. *Scientific Reports*, *5*(13293). doi: 10.1038/srep13293

Menke, A., & Giehl, K. (2012). Regulation of adherens junctions by Rho GTPases and p120-catenin. *Archives of Biochemistry and Biophysics*, *524*(1), 48–55. doi:10.1016/j.abb.2012.04.019

Micol, V., Sánchez-Piñera, P., Villalaín, J., de Godos, a, & Gómez-Fernández, J. C. (1999). Correlation between protein kinase C alpha activity and membrane phase behavior. *Biophysical Journal*, *76*(2), 916–927. doi:10.1016/S0006-3495(99)77255-3

Mitchell, T.J., Andrew, P.W., Saunders, F.K., Smith, A.N., and Boulnois, G.J. (1991). Complement activation and antibody binding by pneumolysin via a region of the toxin

homologous to a human acute-phase protein. *Molecular Microbiology 5*(8), 1883-1888. doi: 10.1111/j.1365-2958.1991.tb00812.x

Mitchell, Tim J. "Pneumolysin: Structure, Function, and Role in Disease." *The Comprehensive Sourcebook of Bacterial Protein Toxins*. By J. E. Alouf and Michel R. Popoff. 3rd ed. Amsterdam: Elsevier, 2006. 680-699. Print.

Mitchell, A. M., and T. J. Mitchell. "*Streptococcus Pneumoniae*: Virulence Factors and Variation." *Clinical Microbiology and Infection* 16.5 (2010): 411-418. *Wiley Online Library*. Wiley Science, 2 Feb. 2010. Web. 01 Oct. 2012. <http://onlinelibrary.wiley.com/doi/10.1111/j.1469-0691.2010.03183.x/abstract;jsessionid=5152B357668BC0E2330C16047DBCFFE4.d03t01>.

Morgan, P. J., Hyman, S. C., Byron, O., Andrew, P. W., Mitchell, T. J., & Rowe, a J. (1994). Modeling the bacterial protein toxin, pneumolysin, in its monomeric and oligomeric form. *The Journal of biological chemistry*, *269*(41), 25315–25320. Retrieved from http://www.ncbi.nlm.nih.gov/pubmed/7929224

Murray, Patrick R., Ken S. Rosenthal, and Michael A. Pfaller. "Chapter 22: Streptococcus." *Medical Microbiology*. 6th ed. Philadelphia: Elsevier, 2009. 225-242. Print.

Nelson, A. L., Roche, A. M., Gould, J. M., Chim, K., Ratner, A. J., & Weiser, J. N. (2007). Capsule enhances pneumococcal colonization by limiting mucus-mediated clearance. *Infection and immunity*, *75*(1), 83–90. doi:10.1128/IAI.01475-06

Paton, J.C., Rowan-Kelly, B. and Ferrante, A. (1984). Activation of Human Complement by

the Pneumococcal Toxin Pneumolysin. *Infection and Immunity*, *43*(3), 1085-1087. Retrieved from www.ncbi.nlm.nih.gov/pmc/articles/PMC264298.

Paton, J. C., Lock, R. a, Lee, C. J., Li, J. P., Berry, a M., Mitchell, T. J., … Boulnois, G. J. (1991). Purification and immunogenicity of genetically obtained pneumolysin toxoids and their conjugation to *Streptococcus pneumoniae* type 19F polysaccharide. *Infection and Immunity*, *59*(7), 2297–2304. Retrieved from http://www.pubmedcentral.nih.gov/articlerender.fcgi?artid=258010&tool=pmcentrez&rendertype=abstract

Pearce, B. J., Iannelli, F., & Pozzi, G. (2002). Construction of new unencapsulated (rough) strains of *Streptococcus pneumoniae*. *Research in Microbiology*, *153*(4), 243–247. Retrieved from http://www.ncbi.nlm.nih.gov/pubmed/12066896

Ratner, A. J., Hippe, K. R., Aguilar, J. L., Bender, M. H., Nelson, A. L., & Weiser, J. N. (2006). Epithelial cells are sensitive detectors of bacterial pore-forming toxins. *The Journal of biological chemistry*, *281*(18), 12994–12998. doi:10.1074/jbc.M511431200

Rossum, A. M. C. Van, Lysenko, E. S., & Weiser, J. N. (2005). Host and Bacterial Factors Contributing to the Clearance of colonization by *Streptococcus pneumoniae* in a Murine Model, *73*(11), 7718–7726. doi:10.1128/IAI.73.11.7718

Saito, M., Tucker, D. K., Kohlhorst, D., Niessen, C. M., & Kowalczyk, A. P. (2012). Classical and desmosomal cadherins at a glance. *Journal of Cell Science*, *125*(Pt 11), 2547–2552. doi:10.1242/jcs.066654

Shin, H.-S., Yoo, I.-H., Kim, Y.-J., Kim, H.-B., Jin, S., & Ha, U.-H. (2010). MKP1 regulates the induction of inflammatory response by pneumococcal pneumolysin in human

epithelial cells. *FEMS Immunology and Medical Microbiology*, *60*(2), 171–178. doi:10.1111/j.1574-695X.2010.00733.x

Shoma, S., Tsuchiya, K., Kawamura, I., Nomura, T., Hara, H., Uchiyama, R., Daim, S., et al. (2008). Critical involvement of pneumolysin in production of interleukin-1alpha and caspase-1-dependent cytokines in infection with *Streptococcus pneumoniae* in vitro: a novel function of pneumolysin in caspase-1 activation. *Infection and immunity*, *76*(4), 1547–1557. doi:10.1128/IAI.01269-07

Srivastava, A., Henneke, P., Visintin, A., Morse, S. C., Martin, V., Watkins, C., Paton, J. C., et al. (2005). The Apoptotic response to Pneumolysin Is Toll-Like Receptor 4 Dependent and Protects against Pneumococcal Disease, *73*(10), 6479–6487. doi:10.1128/IAI.73.10.6479

Srivastava, K., Shao, B., & Bayraktutan, U. (2013). PKC-β exacerbates in vitro brain barrier damage in hyperglycemic settings via regulation of RhoA/Rho-kinase/MLC2 pathway. *Journal of cerebral blood flow and metabolism : official journal of the International Society of Cerebral Blood Flow and Metabolism*, *33*(12), 1928–1936. doi:10.1038/jcbfm.2013.151

Sung, C.K., Li, H., Claverys, J.P. and Morrison, D.A. (2001). An *rpsL* Cassette, Janus, for Gene Replacement through Negative Selection in *Streptococcus pneumoniae*. *Applied and Environmental Microbiology*, *67*(11), 5190-5196. doi:10.1128/AEM.67.11.5190-5196.2001

Tettelin, H., Nelson, K.E., Paulsen, I.T., Elsen, J.A., Read, T.D., Peterson,S., Heidelberg, J., DeBoy, R.T., Haft, D.H., Dodson, R.J., Durkin, A.S., Gwinn, M., Kolonav, J.F., Nelson, W.C., Peterson, J.D., Umavam, L.A., White, O., Salzberg, S.L., Lewis, M.R., Radune,

D., Holtzapple, E., Khouri, H., Wolf, A.M., Uterback, T.R., Hansen, C.L., McDonald, L.A. Feldblvum, T.V., Angiuoli, S., Dickinson, T., Hickey, E.K., Holt, I.E., Loftus, B.J., Yang, F., Smith, H.O., Venter, J.C., Dougherty, B.A., Morrison, D.A., Hollingshead, S.K. and Fraser, C.M. (2001). Complete Genome Sequence of a virulent isolate of *Streptococcus pneumoniae*. *Science 293*(5529), 498-506. doi: 10.1126/science.1061217.

Tian, X., Liu, Z., Niu, B., Zhang, J., Tan, T. K., Lee, S. R., … Zheng, G. (2011). E-cadherin/β-catenin complex and the epithelial barrier. *Journal of Biomedicine & Biotechnology*, *2011*, 567305. doi:10.1155/2011/567305

Tilley, S. J., Orlova, E. V, Gilbert, R. J. C., Andrew, P. W., & Saibil, H. R. (2005). Structural basis of pore formation by the bacterial toxin pneumolysin. *Cell*, *121*(2), 247–256. doi:10.1016/j.cell.2005.02.033

Van der Windt, D., Bootsma, H. J., Burghout, P., van der Gaast-de Jongh, C. E., Hermans, P. W. M., & van der Flier, M. (2012). Nonencapsulated *Streptococcus pneumoniae* resists extracellular human neutrophil elastase- and cathepsin G-mediated killing. *FEMS Immunology and Medical Microbiology*, *66*(3), 445–448. doi:10.1111/j.1574-695X.2012.01028.x

Wardill, H. R., Gibson, R. J., Logan, R. M., & Bowen, J. M. (2013). TLR4/PKC-mediated tight junction modulation: a clinical marker of chemotherapy-induced gut toxicity? *International Journal of cancer. Journal International du cancer*, 1–26. doi:10.1002/ijc.28656

Yamaguchi, M., Terao, Y., Mori-Yamaguchi, Y., Domon, H., Sakaue, Y., Yagi, T., … Kawabata, S. (2013). *Streptococcus pneumoniae* invades erythrocytes and utilizes them

to evade human innate immunity. *PloS One*, *8*(10), e77282. doi:10.1371/journal.pone.0077282

Zhao, Z. S., Manser, E., Chen, X. Q., Chong, C., Leung, T., & Lim, L. (1998). A conserved negative regulatory region in alphaPAK: inhibition of PAK kinases reveals their morphological roles downstream of Cdc42 and Rac1. *Molecular and Cellular Biology*, *18*(4), 2153–2163. Retrieved from http://www.pubmedcentral.nih.gov/articlerender.fcgi?artid=121452&tool=pmcentrez&rendertype=abstract

"General Information on Pneumococcal Disease." *Public Health England*. Public Health England, 23 Apr. 2013. Web. 25 May 2013. <http://www.hpa.org.uk/web/HPAweb&HPAwebStandard/HPAweb_C/1203008864027>.

"PATH Vaccine Resource Library: Pneumococcus (Streptococcus Pneumoniae)." *PATH Vaccine Resource Library: Pneumococcus (Streptococcus Pneumoniae)*. PATH, Aug. 2012. Web. 25 May 2013. <http://www.path.org/vaccineresources/pneumococcus-info.php>.

"Pneumonia." *WHO*. World Health Organization, Aug. 2012. Web. 02 Oct. 2012. <http://www.who.int/mediacentre/factsheets/fs331/en/index.html>.

"Pneumococcal Vaccine." *NHS Pneumococcal Vaccination*. National Health Service, 26 Mar. 2012. Web. 25 May 2013. <http://www.nhs.uk/conditions/vaccinations/pages/pneumococcal-vaccination.aspx>.

"Streptococcus Pneumoniae (Pneumococcus)." *WHO*. World Health Organization, n.d.

Web. 25 May 2013.

<http://www.who.int/immunization_delivery/new_vaccines/pneumo/en/index.html>.